

Explore fluid/wave patterns in ducts

Jiaqi_Wang

2020/11/23



上海交通大學

SHANGHAI JIAO TONG UNIVERSITY



1

*What is fluid/wave patterns?
Why is it important?*

2.1

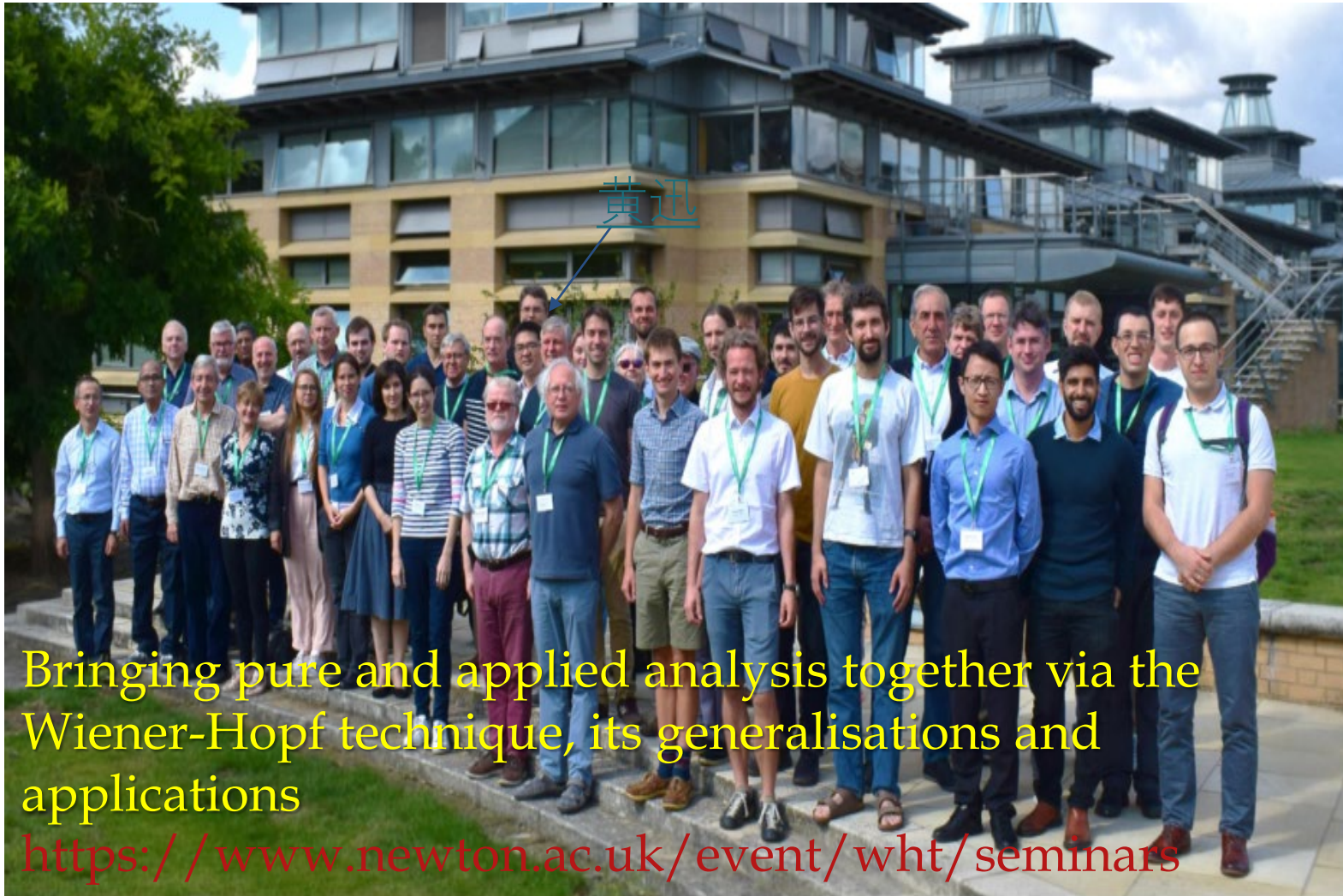
*Is all the emergence of a pattern predictable?
Rayleigh-Bénard instability, Taylor-Couette instability, Duct modes in swirl flow*

2.2

*How to use the patterns in real turbomachinery?
Some Applications.*



My experience of “patterns”



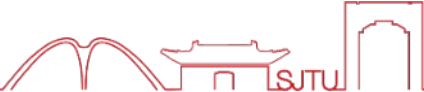
Bringing pure and applied analysis together via the Wiener-Hopf technique, its generalisations and applications

<https://www.newton.ac.uk/event/wht/seminars>



Matthew Colbrook Sheehan Olver
David Abrahams's phd student
Anastasia Kisil & Matthew Priddin

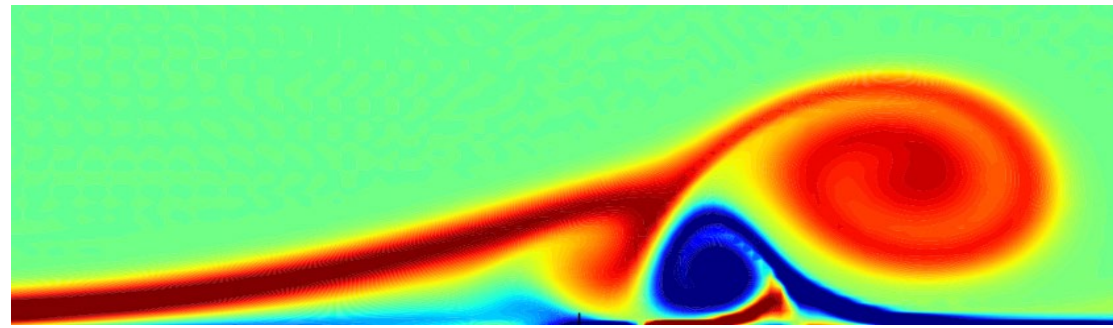
Similarity of patterns



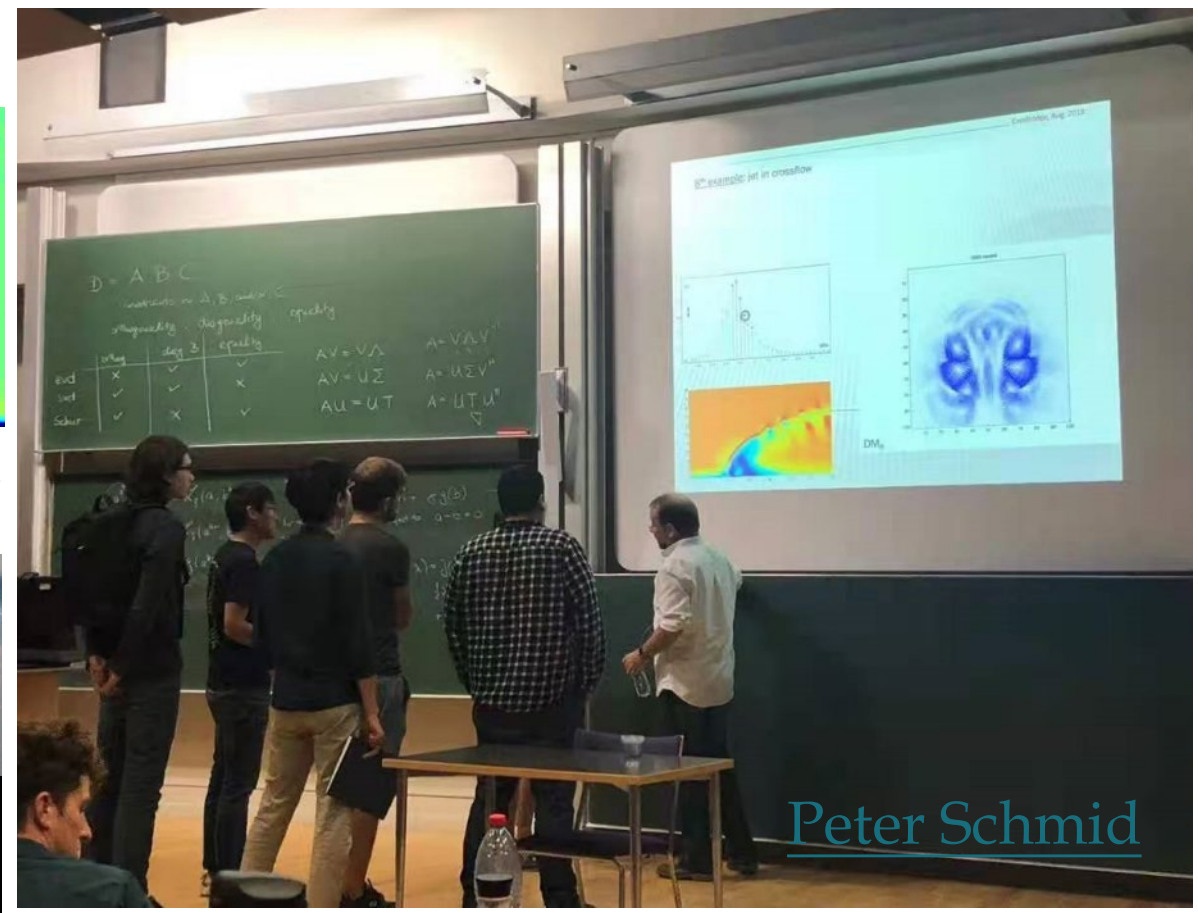
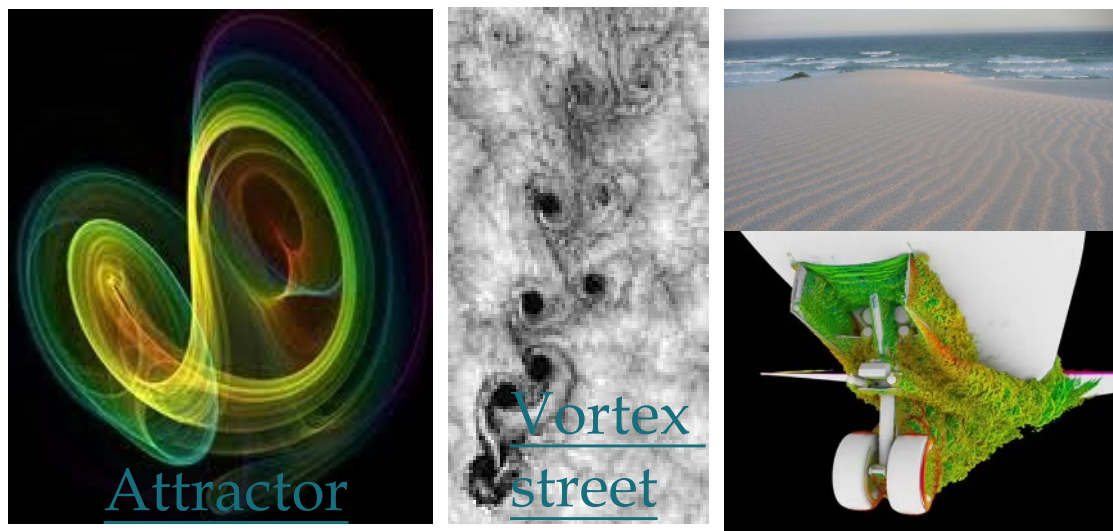
My experience of "flow patterns"



"Flow instability, modelling and control"



<https://fluids.ac.uk/sig/FlowInstability>




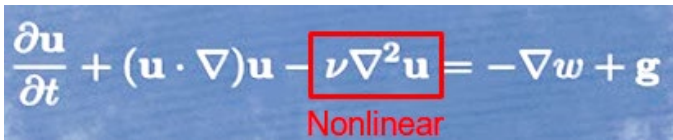
Peter Schmid

At same time, another workshop quietly launched in Cambridge

So, what is pattern?

- Wikipedia: A pattern is a regularity in the world, in human-made design, or in abstract ideas. As such, the elements of a pattern repeat in a predictable manner.

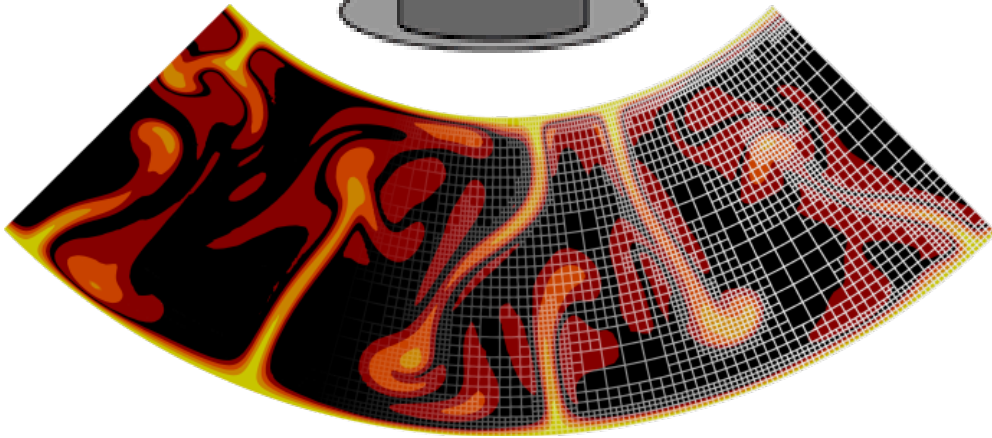
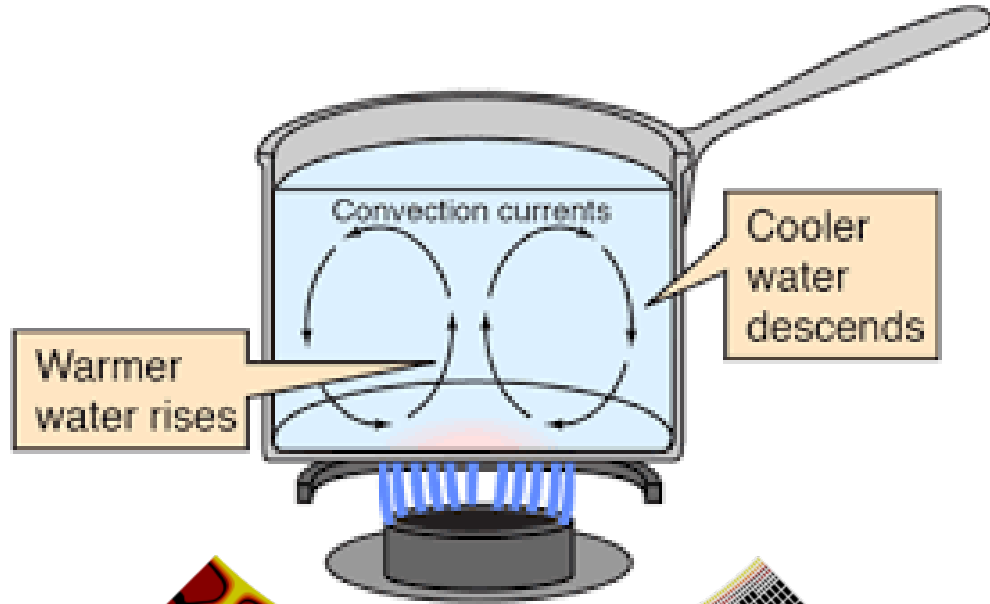
- In chaos theory: $\frac{d}{dt}\mathbf{x}(t) = \mathbf{f}(\mathbf{x}(t), t; \beta)$  Koopman operator $g(\mathbf{x}_{k+1}) = \mathcal{K}_t g(\mathbf{x}_k)$.

- In fluid mechanism: $\frac{\partial \mathbf{u}}{\partial t} + (\mathbf{u} \cdot \nabla) \mathbf{u} - \nu \nabla^2 \mathbf{u} = -\nabla w + \mathbf{g}$  Naiver-stoke equation

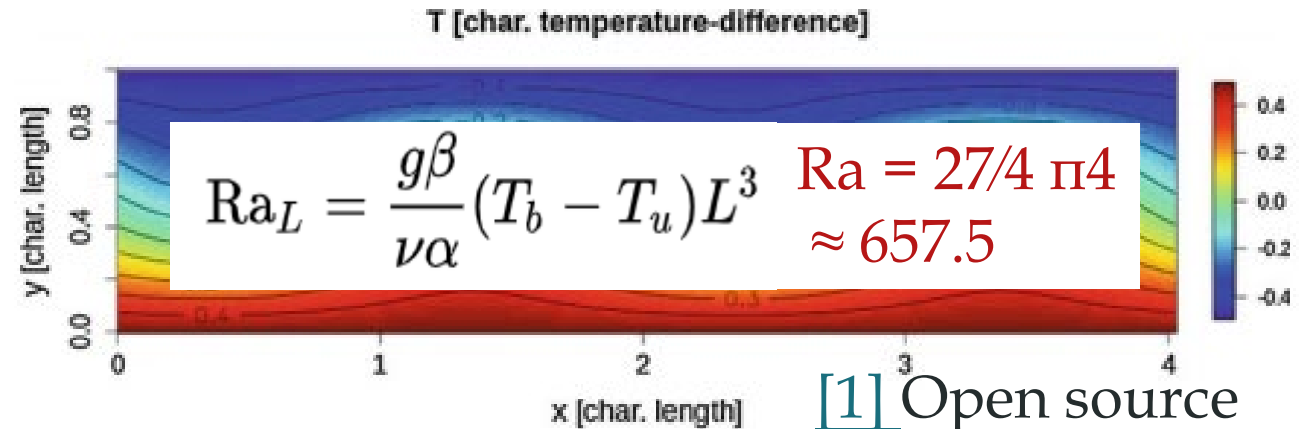
- In mathematician's eyes : $\mathbf{A}\vec{\mathbf{x}} = \lambda\vec{\mathbf{x}}$ $\vec{\mathbf{x}}$ = eigenvector
 λ = eigenvalue

- In engineer's eyes : Resonance / Mode

System in thermodynamic equilibrium



For $\Delta T = (T_{\text{HOT}} - T_{\text{COLD}}) > (\Delta T)_{\text{critical}}$

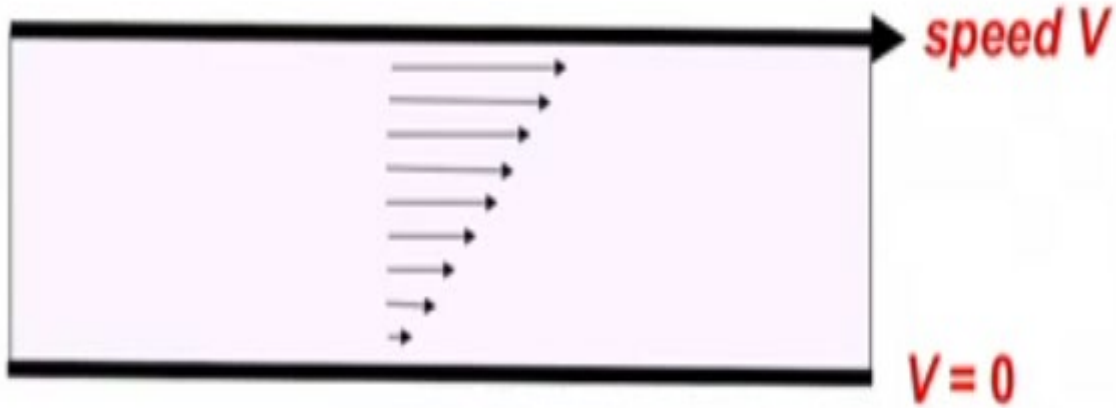


Aspect solver for Earth's Convectic

Is all the emergence of a pattern predictable?



➤ Consider a fluid between two parallel plates:



How large does V have to be for the flow to change the pattern?

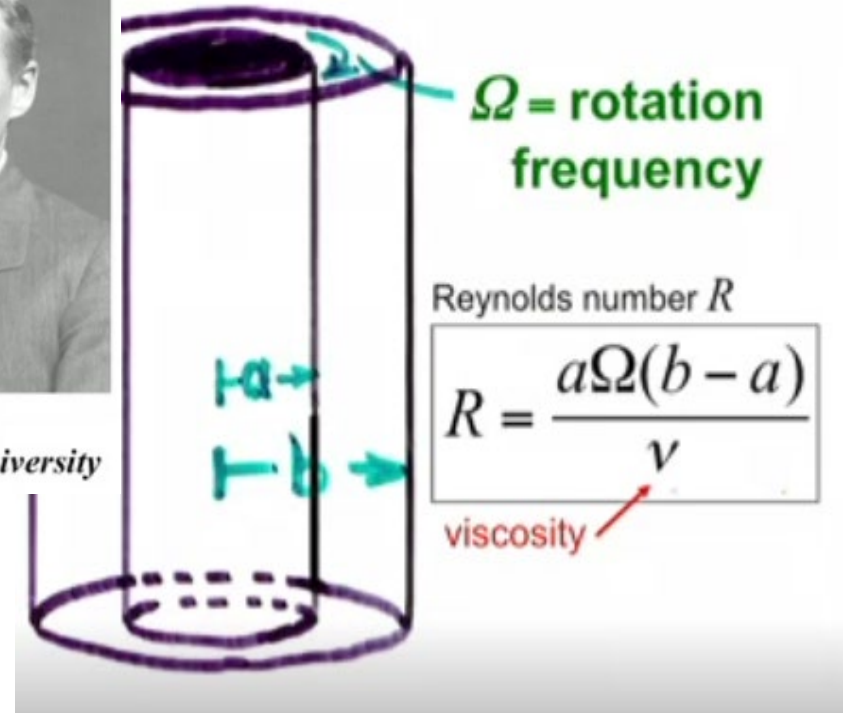
Early 20th century:

All attempts to predict the answer failed.

Fluid between concentric cylinders



G.I. Taylor
Cambridge University



Is all the emergence of a pattern predictable?



Emergence of a pattern: $R > R_c$ Emergence of Taylor vortex pattern



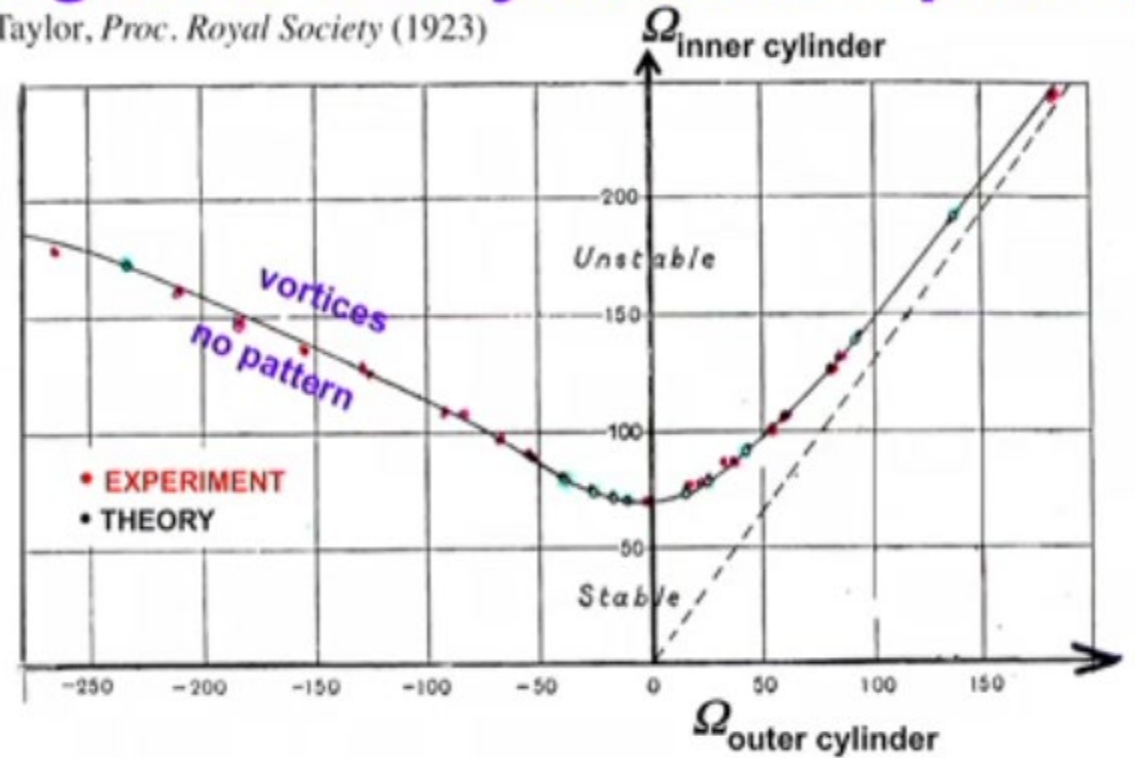
G. I. Taylor
Phil. Trans. Roy. Soc. (1923)

← donut-shaped vortices

↑ vortex pair

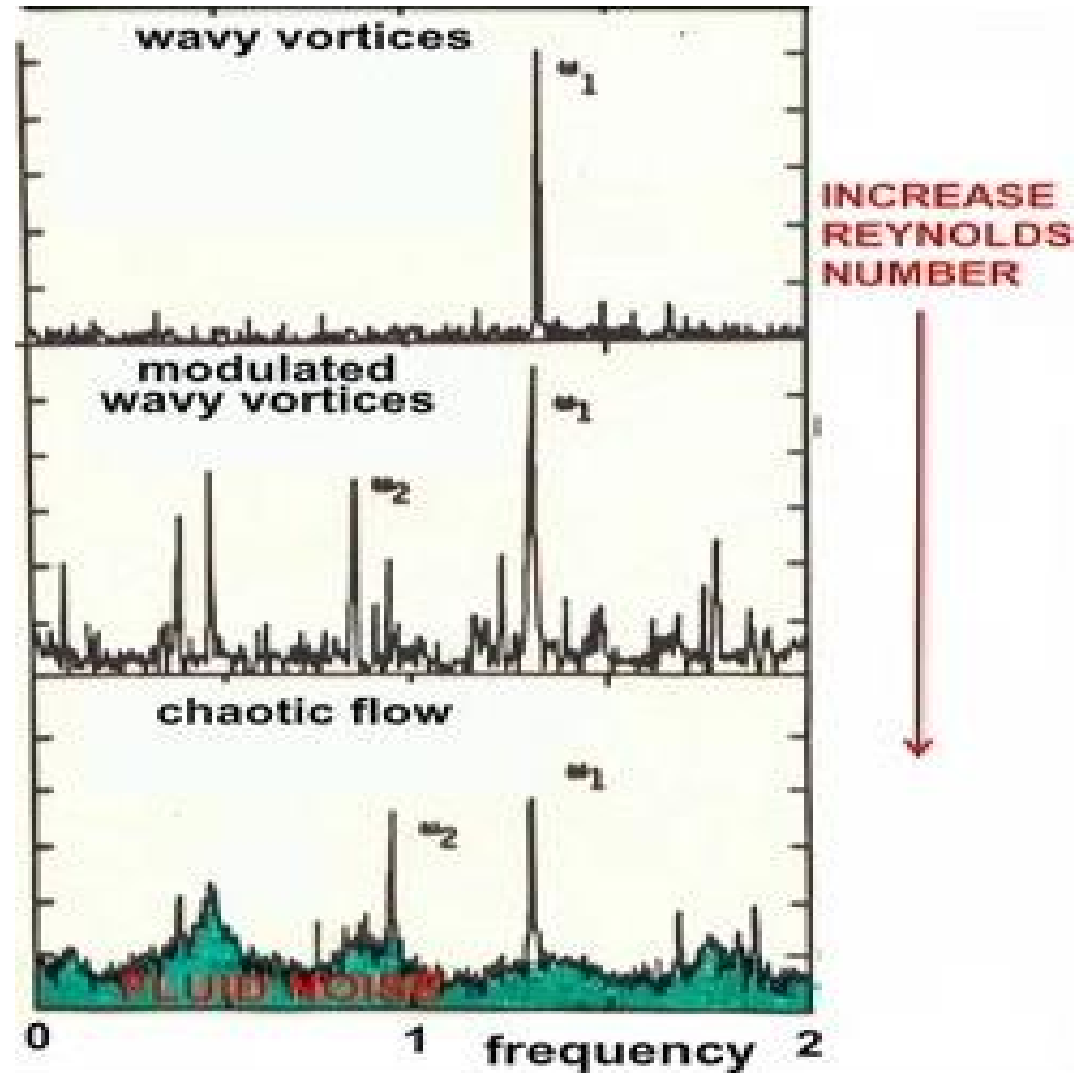
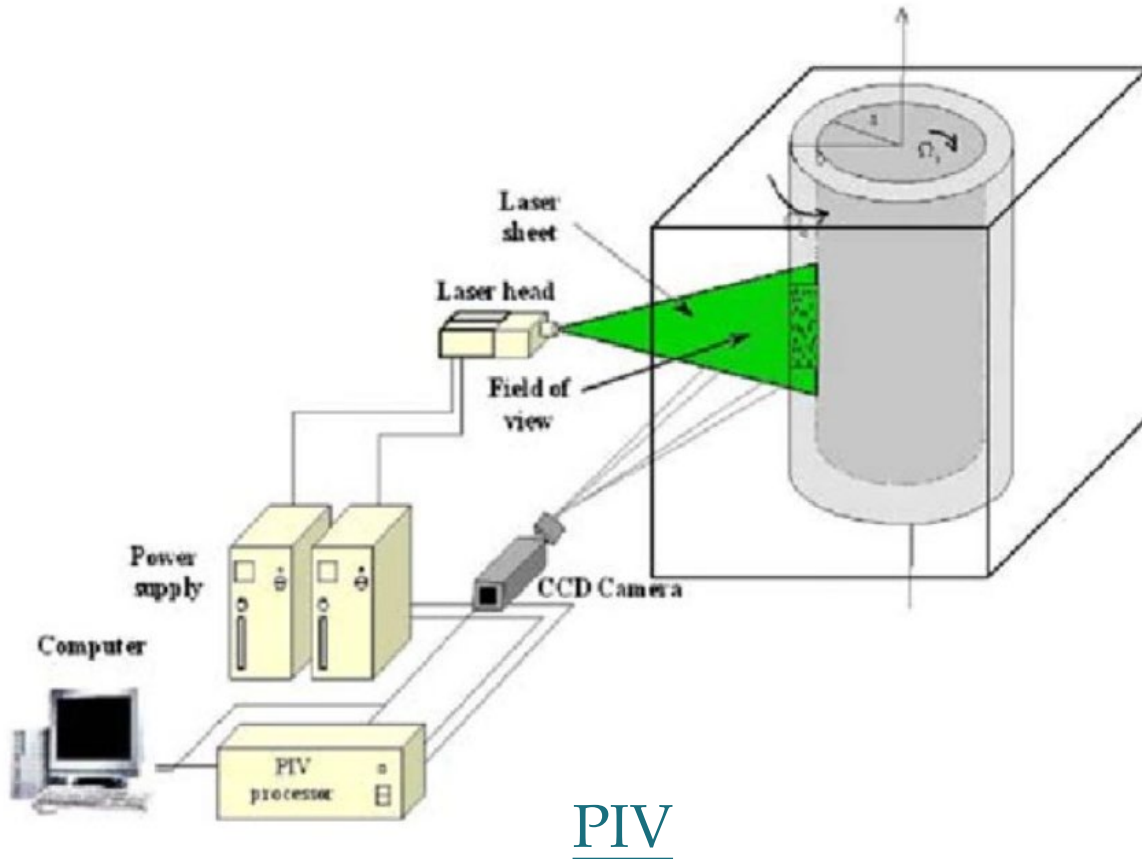
Photo: Andereck, Liu, Swinney
J Fluid Mech. (1985)

G. I. Taylor, *Proc. Royal Society* (1923)



Attempts by Kelvin, Rayleigh, Hopf, Sommerfeld, and others
“to calculate the speed at which any type of flow
would become unstable have failed.”

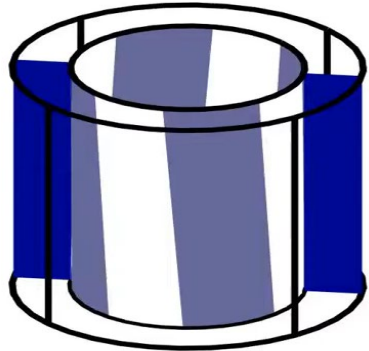
Experiment Taylor–Couette flow system



Explored Taylor–Couette flow system



$$\text{Ta} = \frac{\Omega^2 R_1 (R_2 - R_1)^3}{\nu^2}, \quad \text{Ta} = 0$$

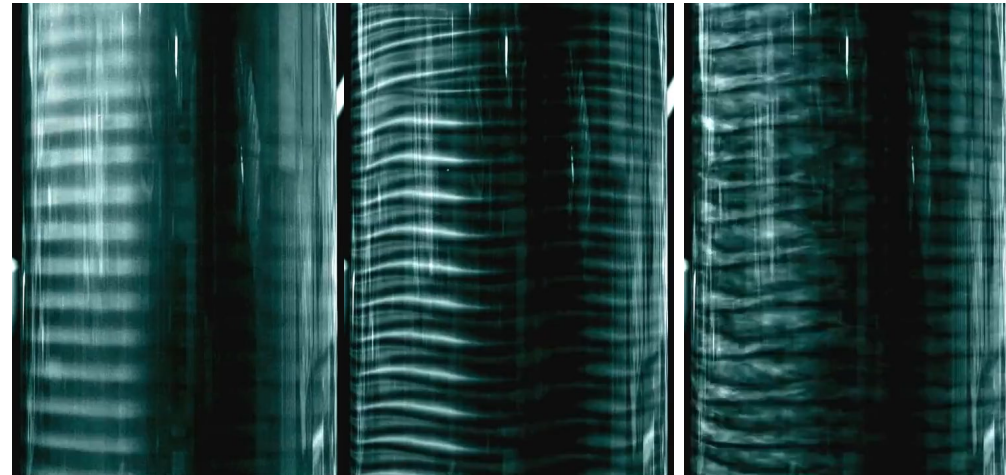
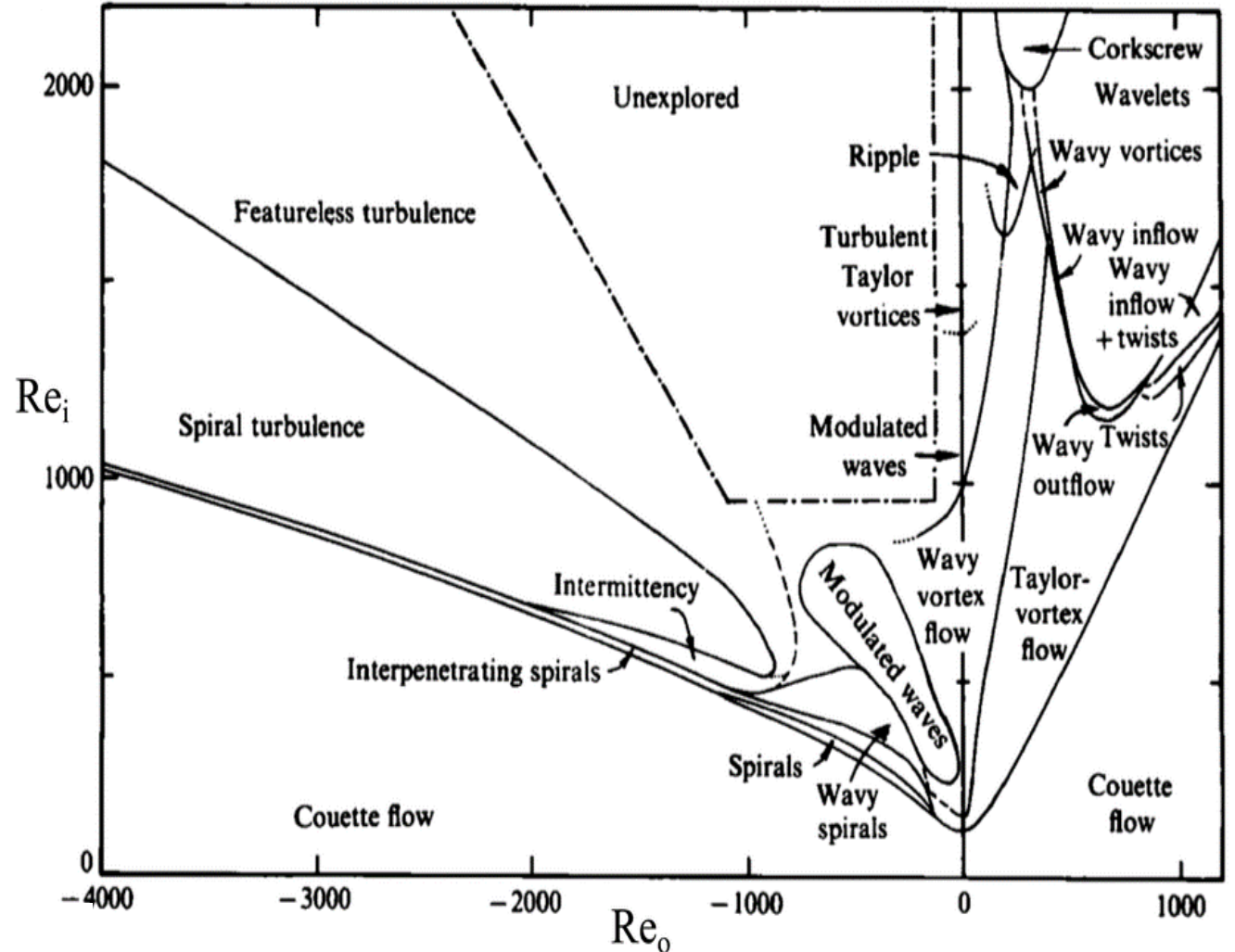


Simulation
by
FEATool
Multiphysics



— Increase Reynolds number —>

[3]: M. A. Fardin-2014



Taylor vortices wavy vortices chaotic flow

[2]: Ruy Ibanez, Phys. Rev. Fluids, 2016

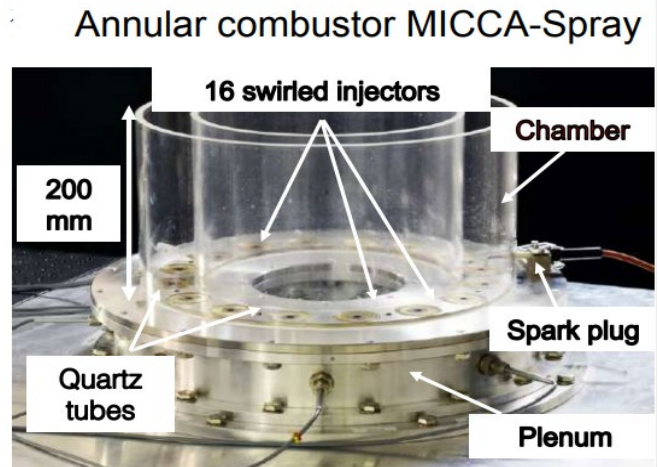
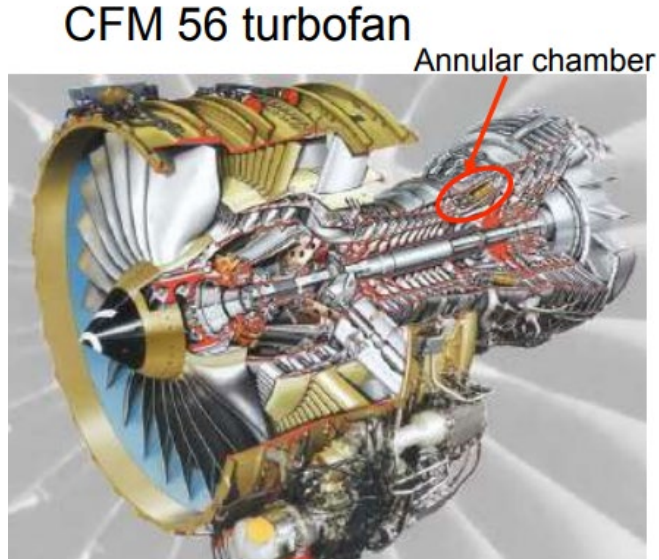


*If patterns exit in more complex fluid dynamical system,
Such like turbomachinery?*

*Well, yes, some could be simplify,
but more others are headache, confusing!*

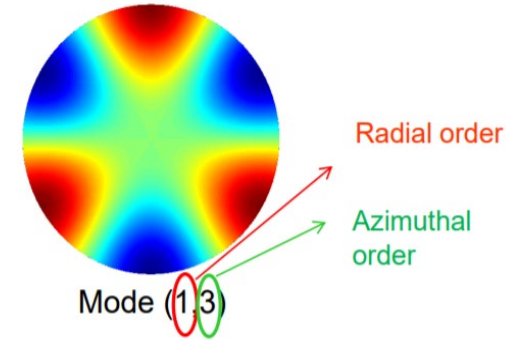
Contact me:
www.deal-ii.com

Combustion instability in ducts



Harmonic modes are governed by a Helmholtz equation

$$\frac{1}{r} \frac{\partial}{\partial r} \left(r \frac{\partial p}{\partial r} \right) + \frac{1}{r^2} \frac{\partial^2 p}{\partial \theta^2} + \frac{\partial^2 p}{\partial z^2} = \frac{1}{c^2} \frac{\partial^2 (rp)}{\partial t^2}$$



Assuming that the wall is rigid, the normal velocity of the pipe wall is 0

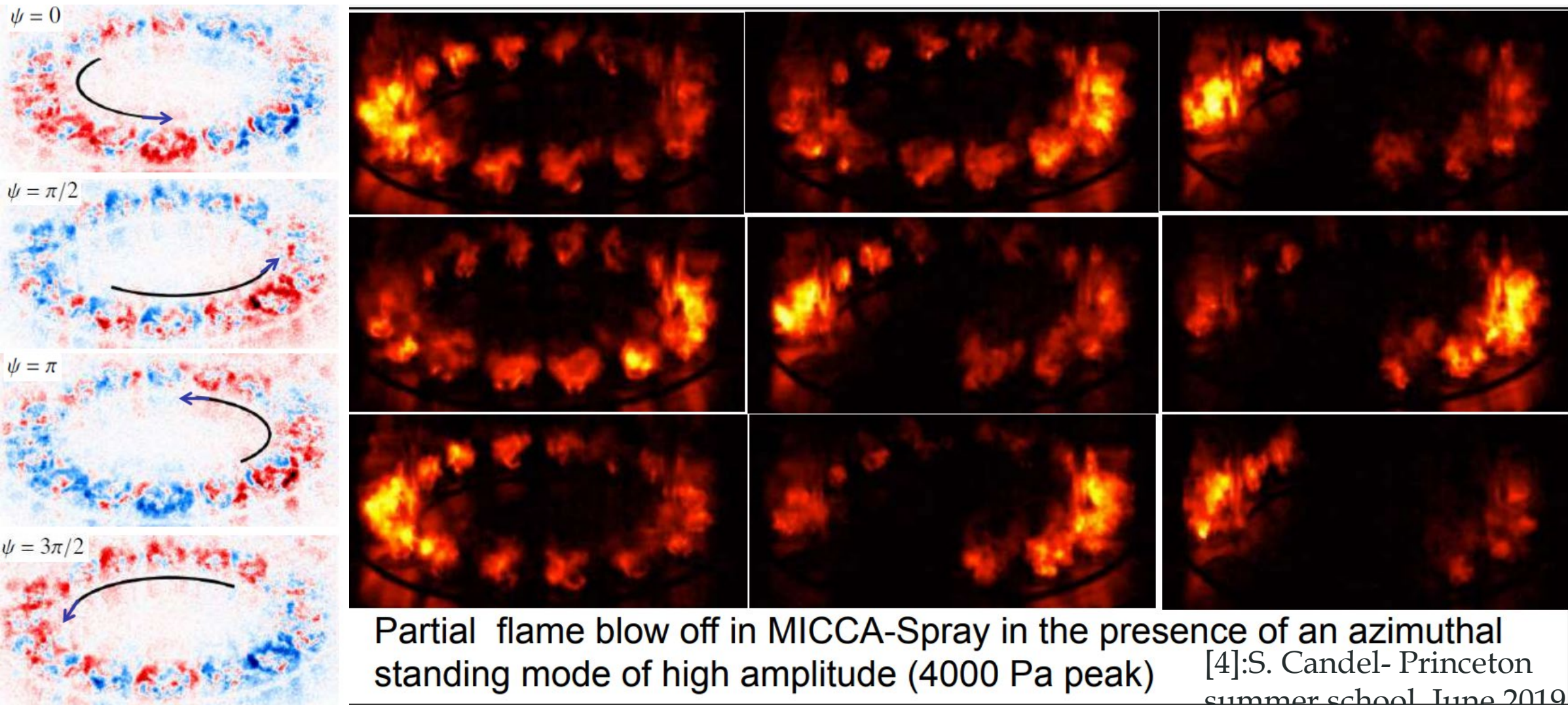
$$u_{rm}|_{r=a} = 0 \Rightarrow \left. \frac{dJ_m(k_{mn}r)}{d(k_{mn}r)} \right|_{r=a} = 0$$

➤ pressure mode superposition :

$$p = \sum_{m=0}^{\infty} \sum_{n=0}^{\infty} A_{mn} J_m(k_{mn}r) \cos(m\theta - \varphi_m) e^{j(\omega t - k_z z)}$$

轴向波数 $k_z = \sqrt{k^2 - k_{mn}^2}$, $k^2 = \frac{\omega^2}{c^2}$
Axial wave number

Combustion rotating modes captured

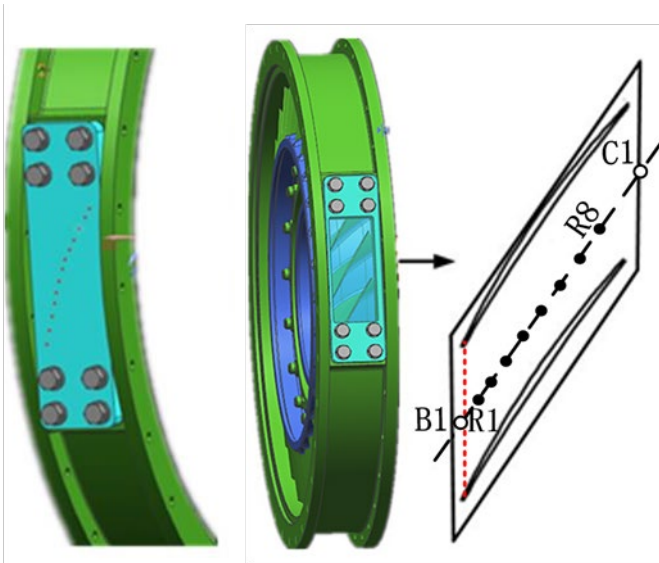


Partial flame blow off in MICCA-Spray in the presence of an azimuthal standing mode of high amplitude (4000 Pa peak) [4]:S. Candel- Princeton summer school, June 2019

Compressor rotating stall



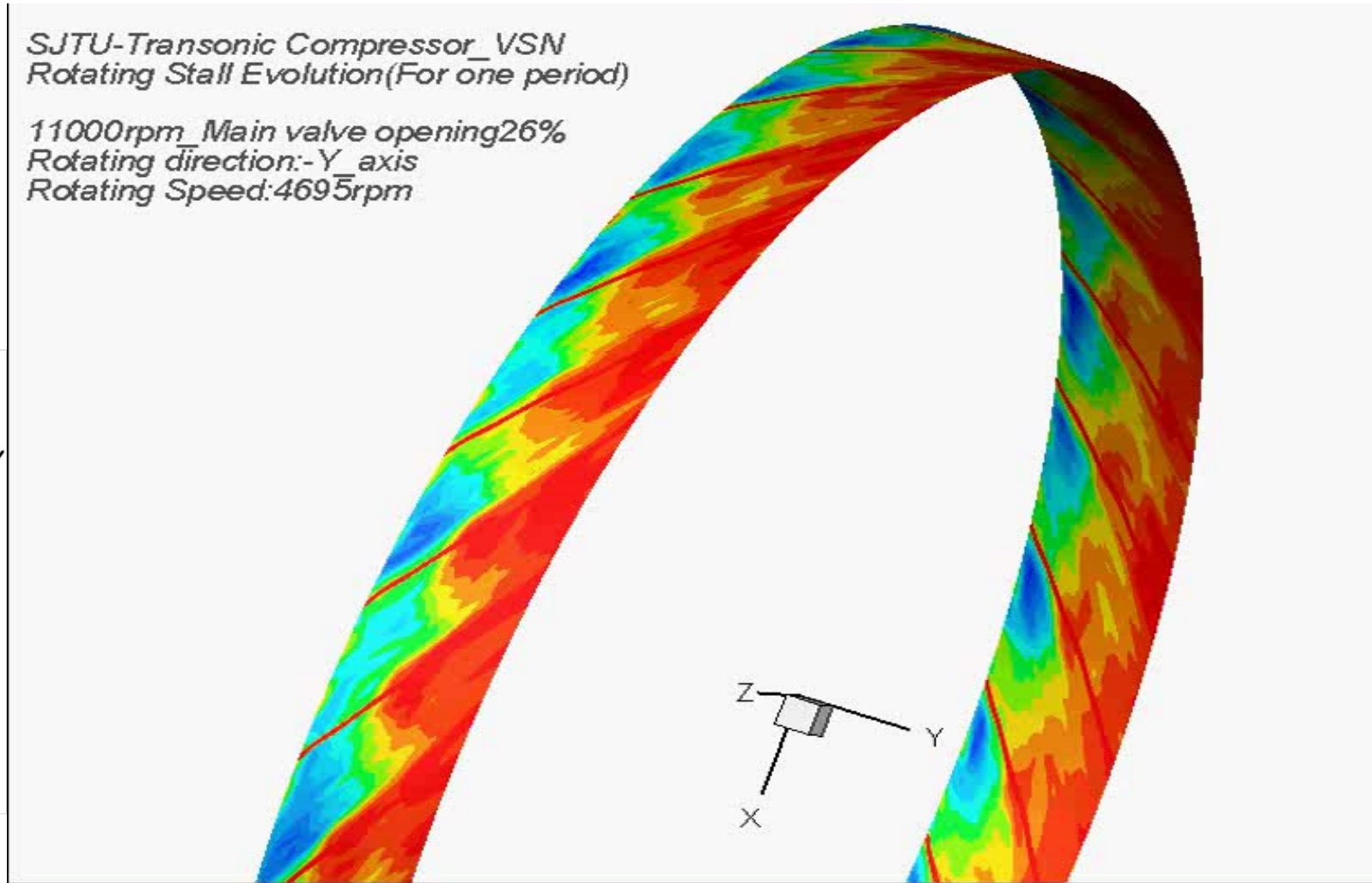
KuliteXCL-062



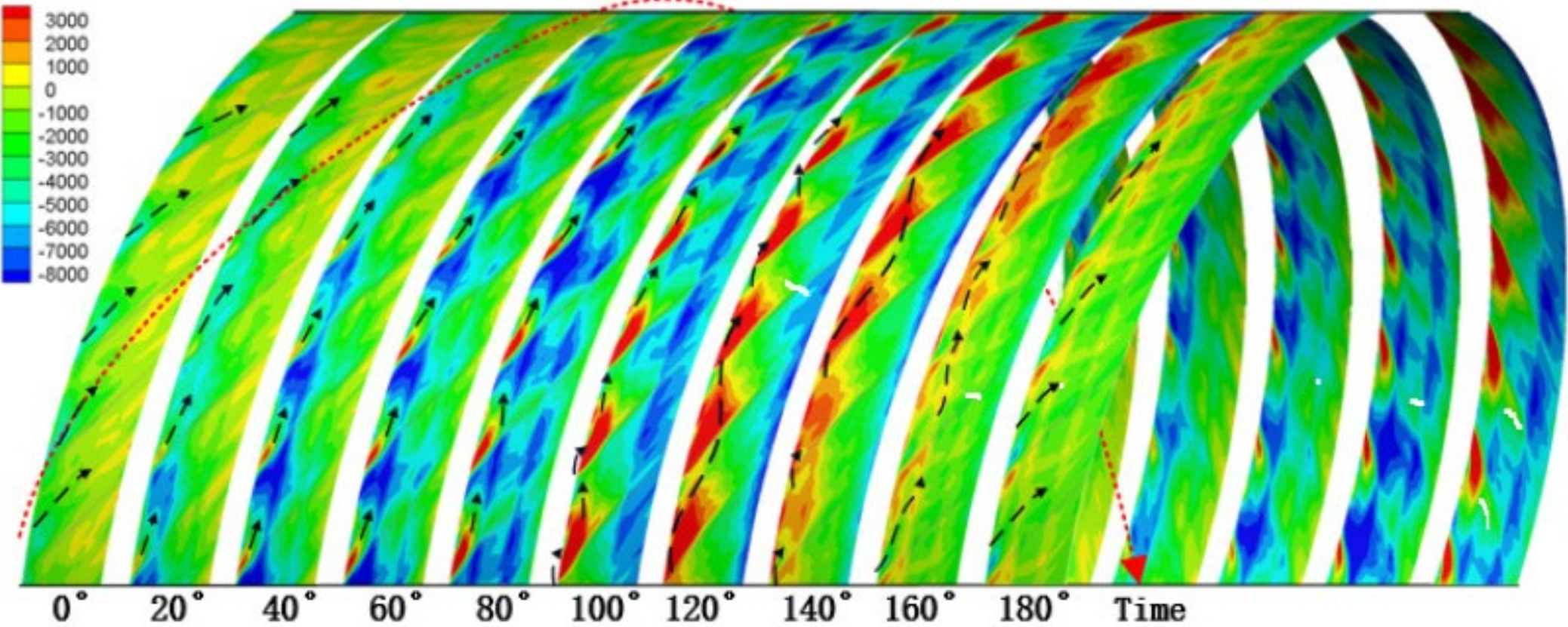
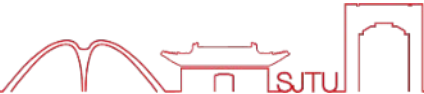
chord measurement layout of rotor

*SJTU-Transonic Compressor_VSN
Rotating Stall Evolution (For one period)*

*11000rpm Main valve opening 26%
Rotating direction: -Y axis
Rotating Speed: 4695rpm*



Pattern of rotating stall



Wave pattern in swirling flow



◆ Should be considered both for combustion and aeroacoustics

⊗ Factor 1: $R1 \leq r \leq R2$

⊗ Factor 2: $u_0(r)$

⊗ Factor 3: $u_\theta(r)$

⊗ Factor 4: Z_t, Z_h

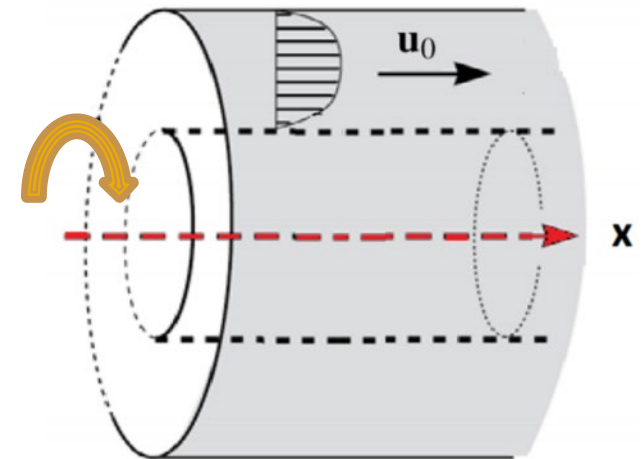
⊗ Factor 5: $s_0(r)$

⊗ Factor 6: $y_1(x) \leq r(x) \leq y_2(x)$

⊗ Factor 7: Conical Duct

⊗ Factor 8: viscosity, turbulence

Realistic
flow



Realistic flow: Eigenvalue



$$\{u, v, w, p, s\}(r, x, \theta, t) = \int \sum_n \int \{U(r), V(r), W(r), P(r), S(r)\} e^{ikx} dke^{in\theta} e^{-i\omega t} d\omega$$

Linear Euler equations :

Wave domain equation

$$\begin{cases} \frac{1}{c_0^2} \frac{D_0 p}{Dt} + \frac{\rho_0 U_\theta^2}{rc_0^2} v + \rho_0 (\nabla \cdot u) = 0 \\ \rho_0 \left(\frac{D_0 u}{Dt} + v \frac{dU_x}{dr} \right) + \frac{\partial p}{\partial x} = 0 \\ \rho_0 \left(\frac{D_0 v}{Dt} - \frac{2U_\theta w}{r} \right) - \frac{U_\theta^2}{r} \rho + \frac{\partial p}{\partial r} = 0 \\ \rho_0 \left(\frac{D_0 w}{Dt} + \frac{v}{r} \frac{d}{dr} (rU_\theta) \right) + \frac{1}{r} \frac{\partial p}{\partial \theta} = 0 \\ \frac{D_0 s}{Dt} + \frac{ds_0}{dr} v = 0 \end{cases}$$



$$\mathbf{A} = \begin{bmatrix} \frac{U_x \hat{\Omega}}{c_0^2 \zeta} i & \left[-\frac{U_x}{c_0^2 \zeta} \frac{dU_x}{dr} + \frac{1}{r\zeta} + \frac{U_\theta^2}{\zeta rc_0^2} \right] + \frac{1}{\zeta} \frac{d}{dr} & \frac{m}{r\zeta} i & -i \frac{\hat{\Omega}}{c_0^2 \rho_0 \zeta} & 0 \\ 0 & -i \frac{\hat{\Omega}}{U_x} & -\frac{2U_\theta}{rU_x} & \frac{1}{\rho_0 U_x} \frac{d}{dr} - \frac{U_\theta^2}{\rho_0 U_x rc_0^2} & \frac{U_\theta^2}{rc_p U_x} \\ 0 & \frac{1}{U_x} \left[\frac{U_\theta}{r} + \frac{dU_\theta}{dr} \right] & -\frac{\hat{\Omega}}{U_x} i & \frac{im}{r\rho_0 U_x} & 0 \\ -\frac{\rho_0 \hat{\Omega}}{\zeta} & \frac{\rho_0}{\zeta} \left[\frac{dU_x}{dr} - \left(\frac{U_\theta^2}{c_0^2} + 1 \right) \frac{U_x}{r} \right] - \frac{\rho_0 U_x}{\zeta} \frac{d}{dr} & -\frac{m\rho_0 U_x}{r\zeta} & i \frac{U_x \hat{\Omega}}{c_0^2 \zeta} & 0 \\ 0 & \frac{1}{U_x} \frac{ds_0}{dr} & 0 & 0 & -i\hat{\Omega} \end{bmatrix} \mathbf{X} = \begin{bmatrix} U \\ V \\ W \\ P \\ S \end{bmatrix}$$

$$\lambda = -ki$$

$$\begin{aligned} \Omega(r) &= \omega - kU_x(r) - \frac{nU_\theta(r)}{r} \\ \hat{\Omega} &= \omega - \frac{nU_\theta}{r}, \zeta = 1 - U_x^2 c_0^2 \end{aligned}$$





Chebyshev Point

$$r_j = \cos \frac{\pi j}{N}, j = 0, \dots, N$$

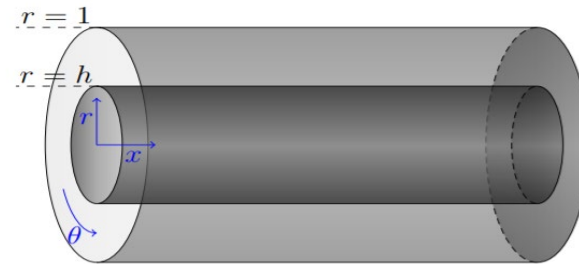
$$f(r) = \sum_{j=0}^N f(r_j) g_j(r)$$

Ingard-Myers boundary condition:

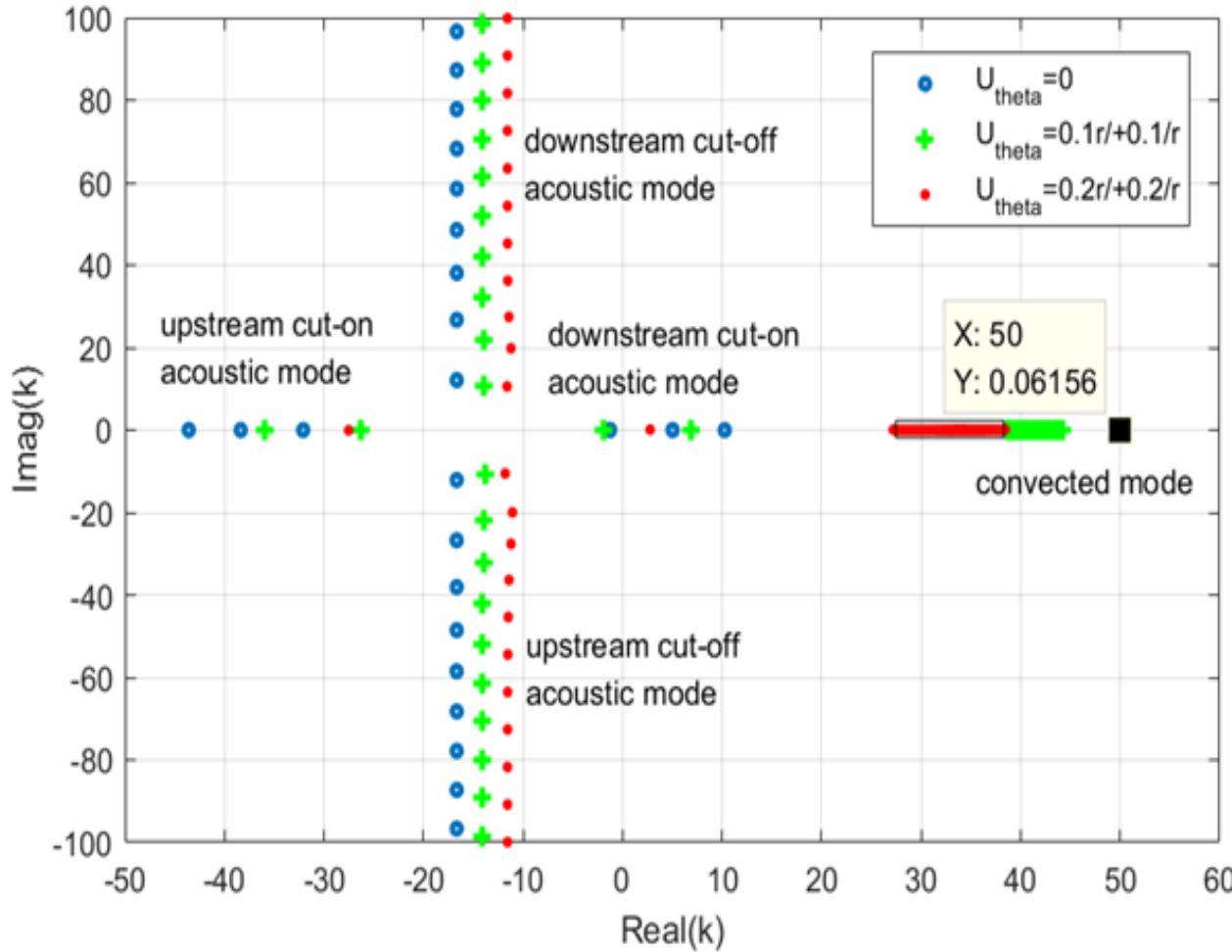
$$\left[\begin{aligned} Z_h \frac{\omega V(h)}{U_x(h)} + \frac{\hat{\Omega}(h)P(h)}{U_x(h)} - kP(h) &= 0 \\ Z_1 \frac{\omega V(1)}{U_x(1)} - \frac{\hat{\Omega}(1)P(1)}{U_x(1)} + kP(1) &= 0 \end{aligned} \right.$$

$$\frac{df(r_i)}{dr} = \sum_{j=0}^N D_{ij} f(r_j), i = 0, \dots, N$$

$$D_{ij} = \begin{cases} \frac{c_i(-1)^{i+j}}{2c_j \sin \frac{\pi}{2N}(i+j) \sin \frac{\pi}{2N}(-i+j)} & i \neq j; i = 0, \dots, N/2; j = 0, \dots, N \\ \frac{-\cos(\frac{\pi i}{N})}{2 \sin^2(\frac{\pi i}{N})} & i = j; i = 1, \dots, N/2; j = 1, \dots, N \\ \frac{2N^2 + 1}{6} & i = j = 0 \\ -D_{N-i, N-j} & i = N/2 + 1, \dots, N; j = 0, \dots, N \end{cases}$$



Explore the pattern from eigenvalue



$h=0.6, w=25, n=15, U_x=0.5$ solid wall

⑤ The eigenvalue is the axial wave number, which reflects the acoustic propagation characteristics of the pipe.

$$\{p\}(r, x, \theta, t) = \int \sum_n \int \{P(r)\} e^{ikx} dk e^{in\theta} e^{-i\omega t} d\omega$$

⑤ (near/pure) acoustic mode

➤ no swirl cut-off line
 $real(k) = -wU_x / (1 - U_x^2)$

⑤ Vortex-dominant (near/pure) convective mode

➤ convected mode
 $-w + kU_x + mU_\theta / r$
 no swirl

⑤ Swirling changes the cutoff and propagation characteristics of pipe acoustic propagation

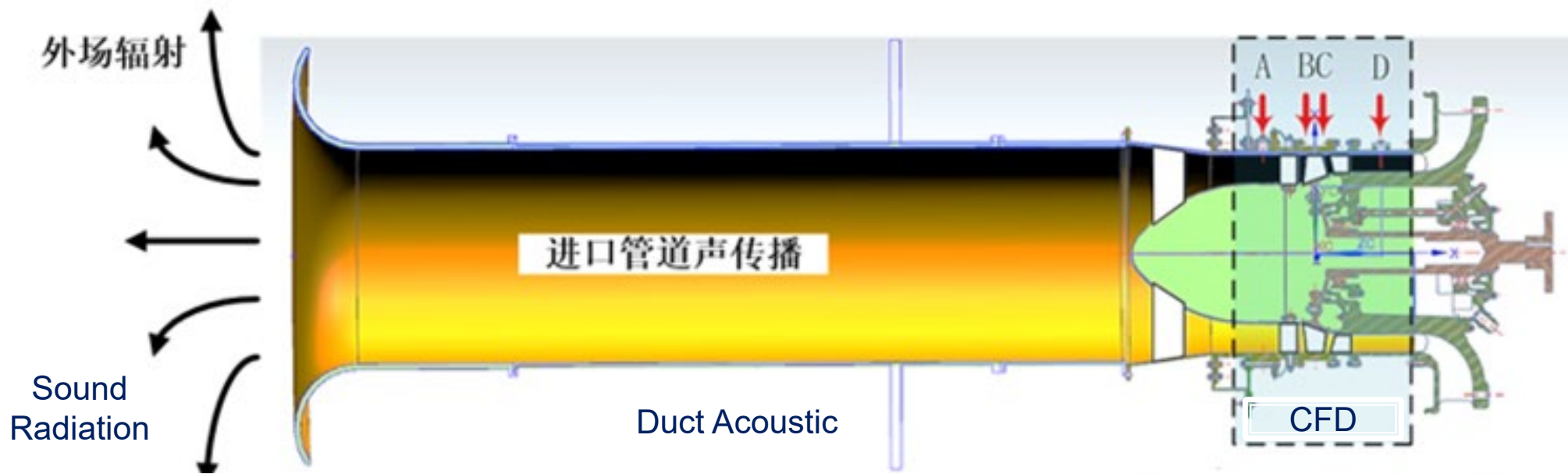
$$\inf_{h < r < 1} \frac{w}{U_x(r)} \leq k \leq \sup_{h < r < 1} \frac{w}{U_x(r)}$$

swirl

$$\inf_{h < r < 1} \frac{w - nU_\theta(r)}{U_x(r)} \leq k \leq \sup_{h < r < 1} \frac{w - nU_\theta(r)}{U_x(r)}$$

⑤ Swirl is one of the acoustic resonance factors in the area of the inlet chute (Copper&Peake 2010 JFM)

Application: Acoustic Analogy



Tonal Blade Noise Modeling

Constructive interference: sound of the total fan = $B \times$ (sound of a single blade)

Bessel function: modulation of the Doppler frequency shift during blade revolution

$$p_{nB} \sim \frac{iBk_{nB}}{4\pi x} e^{ik_{nB}x} \sum_{p=-\infty}^{+\infty} e^{i(nB-p)(\varphi-\pi/2)} J_{nB-p}(k_{nB}R_0 \sin \theta) \left[\bar{F}_{T,p} \cos \theta - \frac{nB-p}{k_{nB}R_0} \bar{F}_{D,p} \right]$$

Sound emitted at BPFHs

Sum over BLHs

Radius where force is applied

Thrust harmonic

Drag harmonic

Acoustic Analogy: realistic flow



Lighthill eq.:

Quadrupole

Dipole

Monopole

$$\rho'(\mathbf{x}, t) = \frac{1}{c_0^2} \int_{-T}^T \int_{V(\tau)} \frac{\partial^2 G}{\partial y_i \partial y_j} T'_{ij} dV d\tau + \frac{1}{c_0^2} \int_{-T}^T \int_{S(\tau)} \frac{\partial G}{\partial y_i} f_i dS(\mathbf{y}) d\tau + \frac{1}{c_0^2} \int_{-T}^T \int_{S(\tau)} \rho_0 V' n \frac{D_0 G}{\partial \tau} dS(\mathbf{y}) d\tau$$

Through the eigenfunction method, the Green's formula for satisfying the boundary conditions of the pipe wall for an infinitely long pipe can be derived.

$$G(\mathbf{y}, \tau | \mathbf{x}, t) = \frac{i}{4\pi} \sum_{m,n} \frac{\Psi_{m,n}(y_2, y_3) \Psi_{m,n}^*(x_2, x_3)}{\Gamma_{m,n}} \times \int_{-\infty}^{+\infty} \frac{\exp \left\{ i \left[w(\tau - t) + \frac{Mk_0}{\beta^2} (y_1 - x_1) + \frac{k_{n,m}}{\beta^2} |y_1 - x_1| \right] \right\}}{k_{n,m}} dw$$

Posson&Peake eq.: (JFM 2012)

Considering the influence of the axial shear and the rotating base flow in the pipeline, the equation is the form of the pressure disturbance under the action of the sixth-order linear operator.

$$F^M \left(\frac{p'}{\rho_0} \right) = S^M$$

$$F^M := \left(\frac{1}{c_0^2} \frac{\bar{D}_0^2}{Dt^2} - \frac{\bar{\partial}^2}{\partial x^2} - \frac{1}{r^2} \frac{\bar{\partial}^2}{\partial \theta^2} \right) \Re^2 + \left(\frac{1}{r} \frac{\bar{D}_0}{Dt} - U'_x \frac{\bar{\partial}}{\partial x} - Y_\theta \frac{\bar{\partial}}{\partial \theta} + \left(\frac{U_\theta^2}{rc_0^2} - \frac{\rho'_0}{\rho_0} \right) \frac{\bar{D}_0}{Dt} \right) \Re \mathbf{T} + \Re \frac{\bar{D}_0}{Dt} \frac{\bar{\partial}}{\partial r} \mathbf{T} - \frac{\bar{D}_0}{Dt} [2U'_x \frac{\bar{\partial}}{\partial x} \frac{\bar{D}_0}{Dt} + 2 \left(\frac{U_\theta}{r} \right)' \frac{\bar{\partial}}{\partial \theta} \frac{\bar{D}_0}{Dt} + \mathfrak{I}'_\theta] \mathbf{T}$$

■ Condition:

- medium (static, uniform);
- Not observed points located in the potential flow field;
- $M < 0.3$.

■ Condition:

- considering the effects of swirl, non-uniform entropy, shear flow, soft wall boundary conditions, etc.;



Possion&Peake's Green function



$$F^M (G(\mathbf{x}, t | \mathbf{x}_0, t_0)) = \delta(\mathbf{x}-\mathbf{x}_0)\delta(t-t_0)$$

$$p(\mathbf{x}, t) = \int (G(\mathbf{x}, t | \mathbf{x}_0, t_0) S^M(\mathbf{x}_0, t)) dx_0 dt_0$$

FFT, expand into cylinder coordination,

$$F^M (G_w(\mathbf{x} | \mathbf{x}_0) e^{-i\omega t}) = \delta(\mathbf{x}-\mathbf{x}_0) e^{-i\omega t} = \delta(x-x_0) \frac{\delta(r-r_0)}{r} \delta(\theta-\theta_0) e^{-i\omega t}$$



$$p(\mathbf{x}, t) = \int (G_w(r, x, \theta | r_0, x_0, \theta_0) S(r_0, x_0, \theta_0)) dx_0 e^{-i\omega t}$$

Gw FFT to Wavenumber domain:

$$G_w(\mathbf{x} | \mathbf{x}_0) = \frac{1}{4\pi^2} \sum_{n=-\infty}^{\infty} e^{in(\theta-\theta_0)} \int_i G_n(r|r_0; w, k) e^{ik(x-x_0)} dk$$

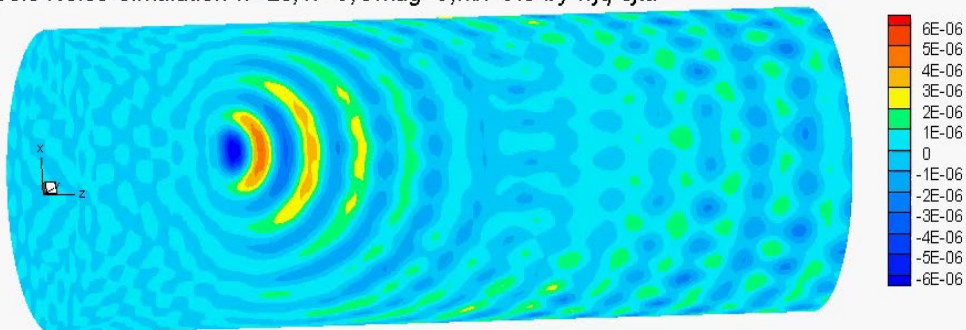
$$G_w \approx \sum_{n=-\infty}^{\infty} e^{in(\theta-\theta_0)} \sum_{Kn^\pm} G_n^m(x, r | x_0, r_0)$$



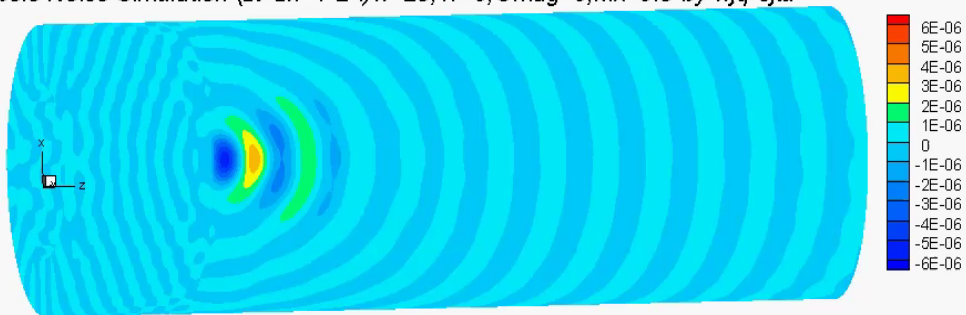
Monopole



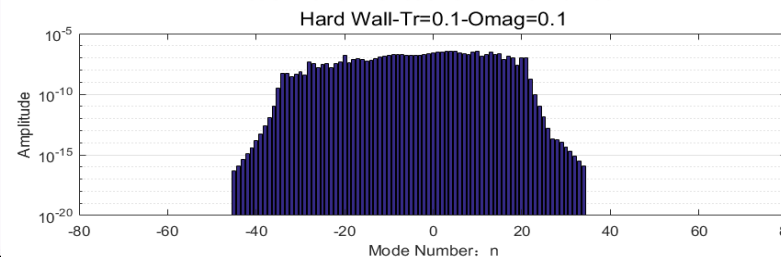
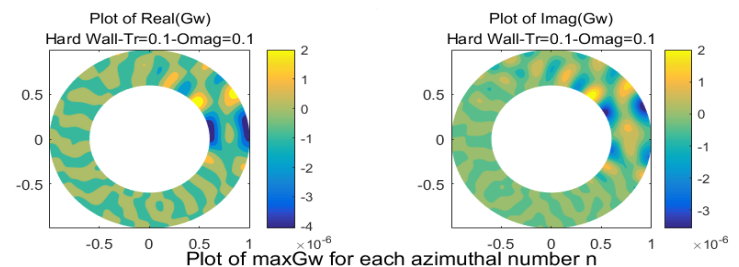
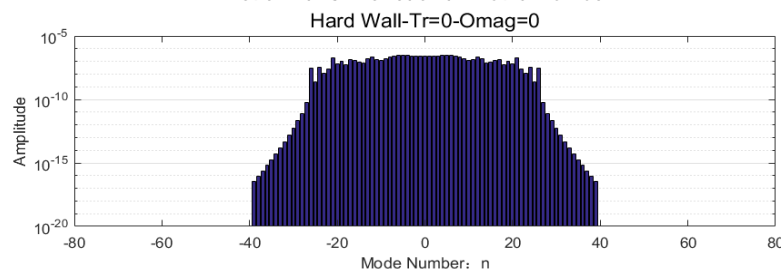
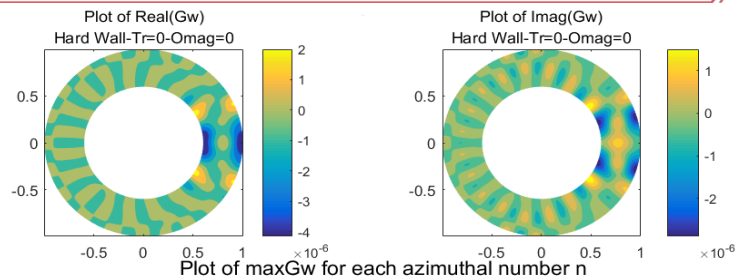
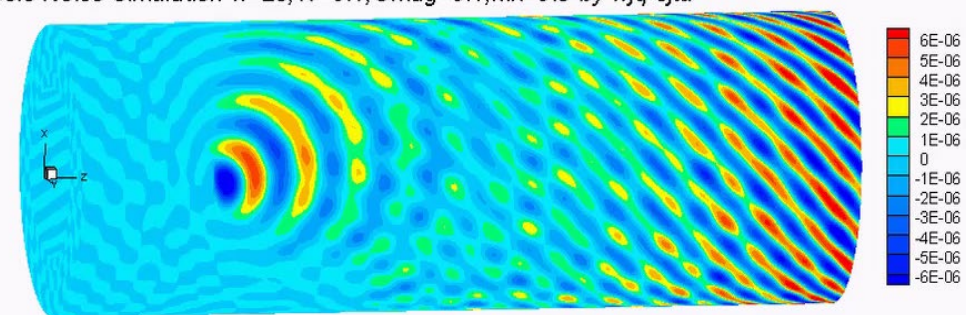
Monopole Noise Simulation $w=25; Tr=0; Omag=0; Mx=0.5$ -by wjq-sjtu



Monopole Noise Simulation ($z_t=z_h=1-2^*$) $w=25; Tr=0; Omag=0; Mx=0.5$ -by wjq-sjtu



Monopole Noise Simulation $w=25; Tr=0.1; Omag=0.1; Mx=0.5$ -by wjq-sjtu



No Swirl

- Sound lining regular mode and reduce noise
- The swirl changes the number of convection waves to enhance a certain order of modes

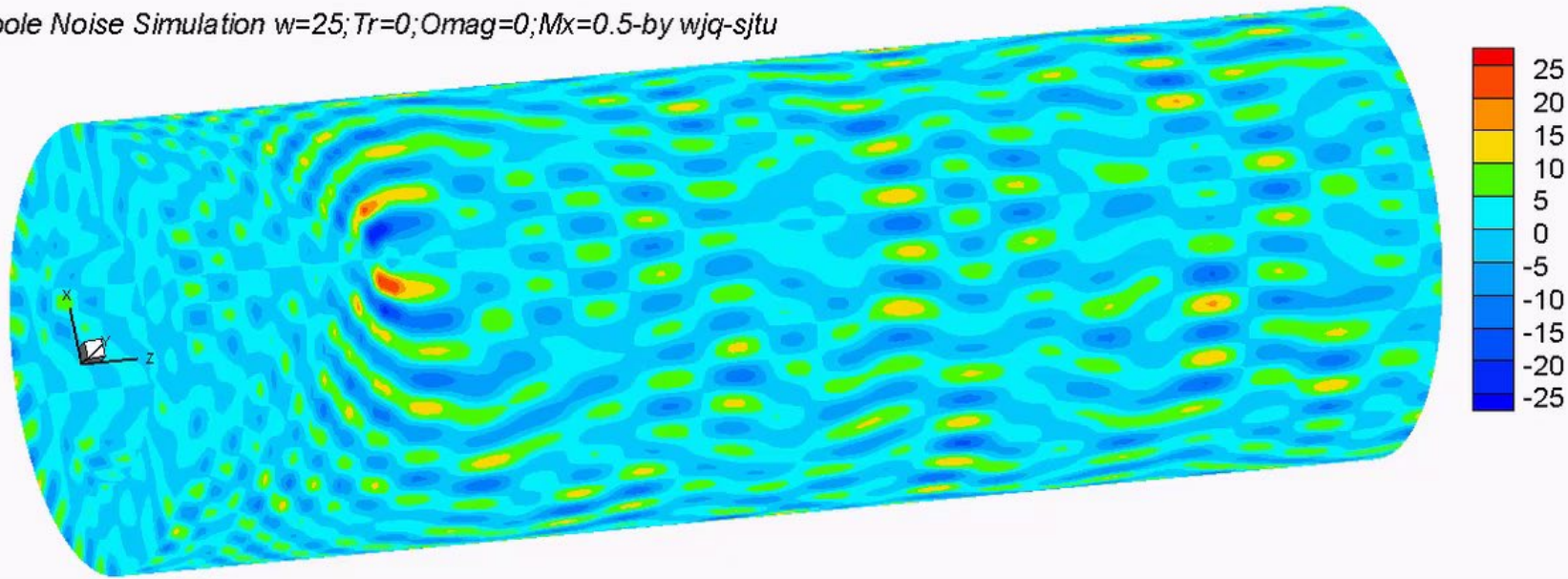
Swirl

- Symmetrical distribution without swirling mode; rapid attenuation after the absolute value of the circumferential mode exceeds 25
- The swirl energy ratio is shifted to the negative direction

Dipole



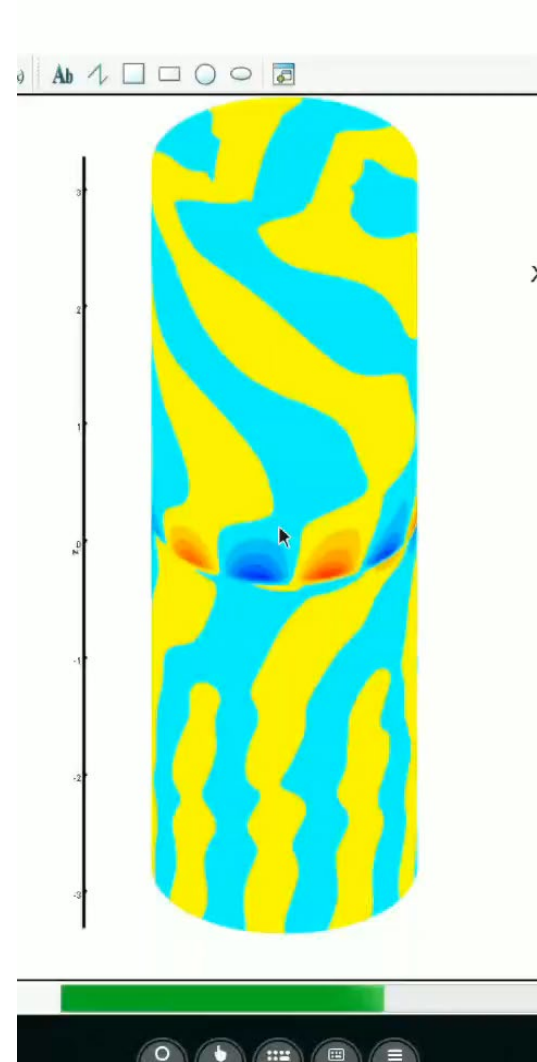
Dipole Noise Simulation $w=25; Tr=0; Omag=0; Mx=0.5$ -by wjq-sjtu



$$p(x_d, r, \theta, t) = \iiint_{\cup_j \Sigma_{B,j}(t_0)} p(\mathbf{x}_{d0}, t_0) \mathcal{T}_0(G(\mathbf{x}_d, t | \mathbf{x}_{d0}, t_0)) d\Sigma_0(t_0) dt_0,$$

$$\mathcal{T}_0(G) = \left[n_{x,j} \mathcal{D}_0^2 \frac{\partial G}{\partial x_{d0}} + n_{\theta,j} \left(\frac{\mathcal{D}_0^2}{r_0} \frac{\partial G}{\partial \theta_0} + 2 \frac{U_\theta}{r_0} \mathcal{R}_{0,1}(G) \right) \right].$$

Rotating



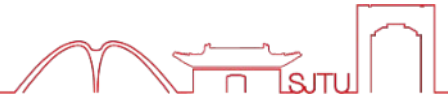
$$p(x_d, r, \theta, t) = - \iint_{\cup_j S_j} \int \Delta P_j(\mathbf{x}_{d0, \mathbf{R}}, t_0) \\ \times \mathcal{T}_0 \left\{ \int_{\omega} \sum_{m \in \mathbb{Z}} \int_k \hat{G}_m(r|k, \omega, r_0) e^{ik(x_d - x_{d0}) + im(\theta - \theta_{0R, j}) - i\omega t + i(\omega - m\Omega_R)t_0} dk d\omega \right\} dt_0 dS_{0, j}.$$

$$\theta_0 = \theta_{0R} + \Omega_R t_0$$

$$p(x_d, r, \theta, t) = 2\pi i \int_{\omega} \sum_{m \in \mathbb{Z}} \int_k \iint_{\cup_j S_j} \Delta \hat{P}_j(\mathbf{x}_{d0, \mathbf{R}}, \omega_m) \mathcal{T}_{m, k, r_0} \left(\hat{G}_m(r|k, \omega, r_0) \right) \\ \times e^{ik(x_d - x_{d0}) + im(\theta - \theta_{0R, j}) - i\omega t} dS_{0, j} dk d\omega.$$

$$\omega_m = \omega - m\Omega_R$$

Fan noise



$$\begin{aligned} \Delta P_j(\mathbf{x}_{d0, \mathbf{R}}, t_0) &= \Delta P(x_{d0}, r_0, \theta_{0R, j}, t_0) = \Delta P\left(x_{d0}, r_0, \theta_{0R, 0} - \frac{2\pi}{B}j, t_0\right) = \Delta P\left(x_{d0}, r_0, \theta_{0R, 0}, t_0 - \frac{2\pi}{B\Omega_R}j\right) \\ &= \Delta P_0\left(\mathbf{x}_{d0, \mathbf{R}}, t_0 - \frac{2\pi}{B\Omega_R}j\right), \end{aligned}$$

$$\Delta P_j(\mathbf{x}_{d0, \mathbf{R}}, t_0) = \sum_{q \in \mathbb{Z}} \Delta \hat{P}_{q, 0}(\mathbf{x}_{d0, \mathbf{R}}) e^{i \frac{2\pi q}{B}j} e^{-i q \Omega_R t_0}$$

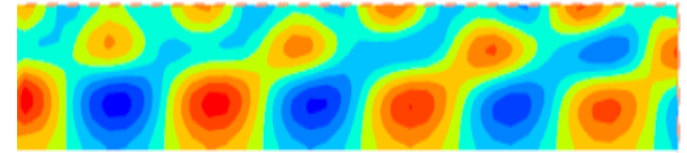
$$p(x_d, r, \theta, t) = \sum_{s \in \mathbb{Z}} \hat{p}_{sB}(x_d, r, \theta) e^{-i s B \Omega_R t} \quad (44a)$$

with

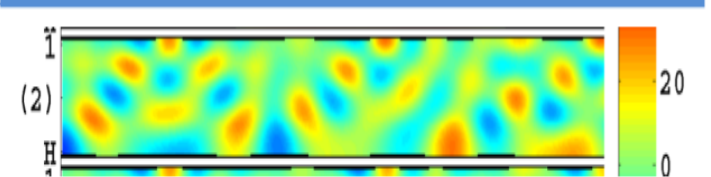
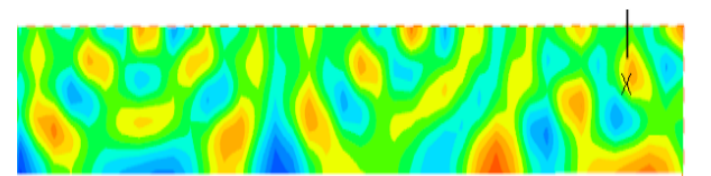
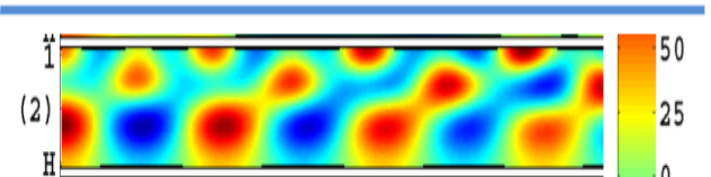
$$\hat{p}_{sB}(\mathbf{x}_d) = 2i\pi B \sum_{q \in \mathbb{Z}} \iint_{S_0} \Delta \hat{P}_{q, 0}(\mathbf{x}_{d0, \mathbf{R}}) \int_k \mathcal{T}_{m, k, r_0} \left(\hat{G}_m(r|k, sB\Omega_R, r_0) \right) e^{ik(x_d - x_{d0})} dk e^{-im\theta_{0R, 0}} dS_{0, 0} e^{im\theta}, \quad (44b)$$

and

$$m = sB - q. \quad (44c)$$



Pressure Field, $m = 16$

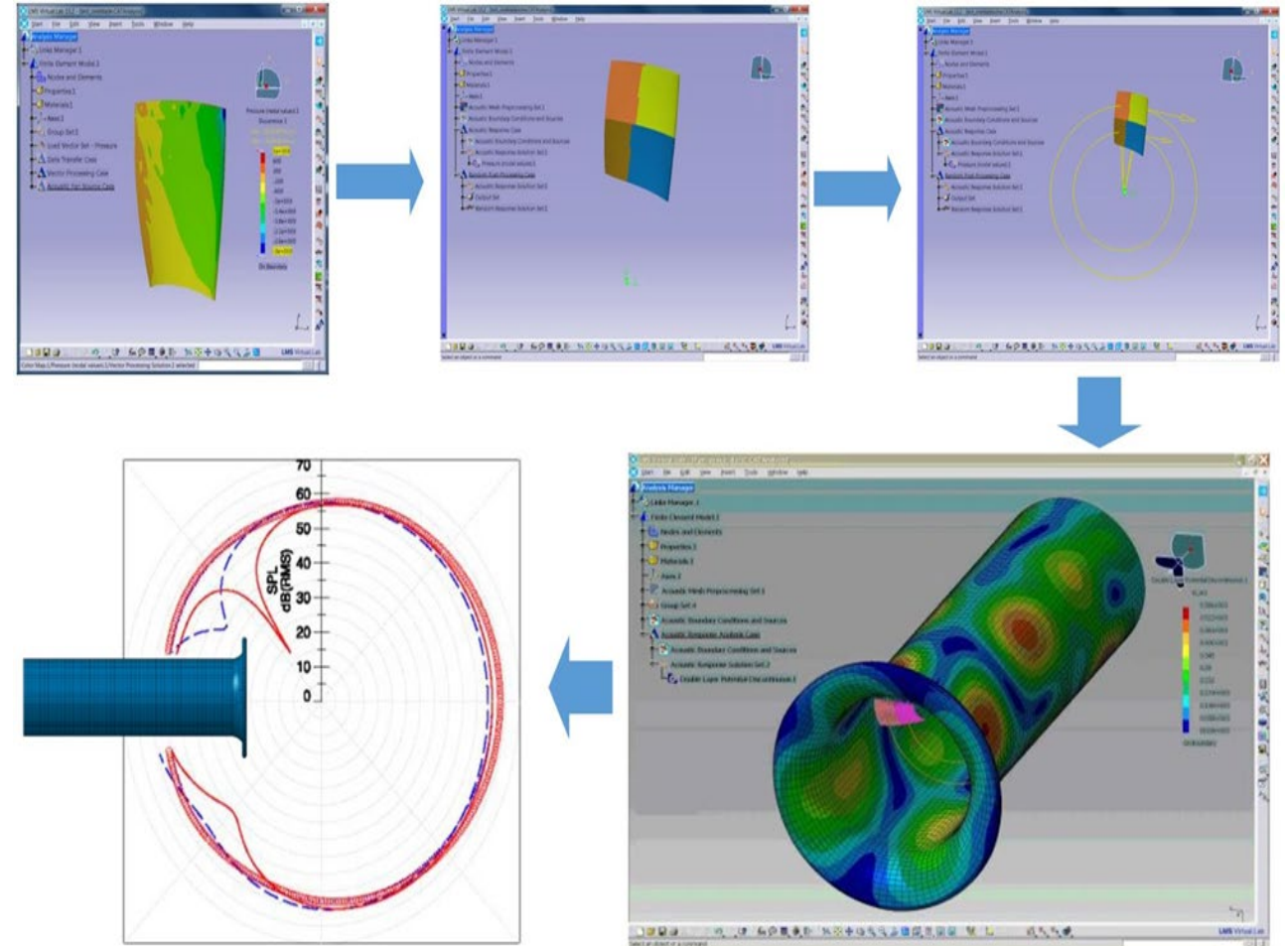


Pressure Field, $m = -16$

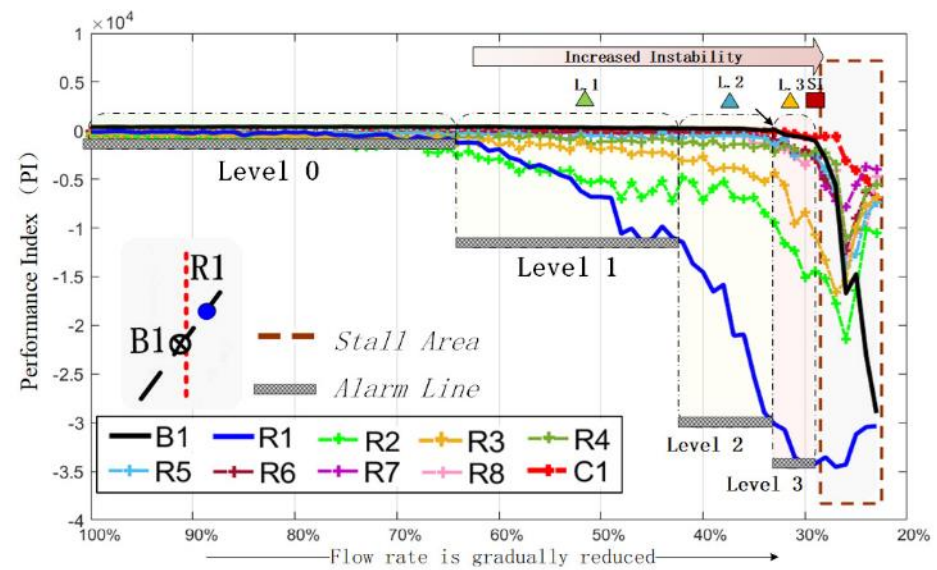
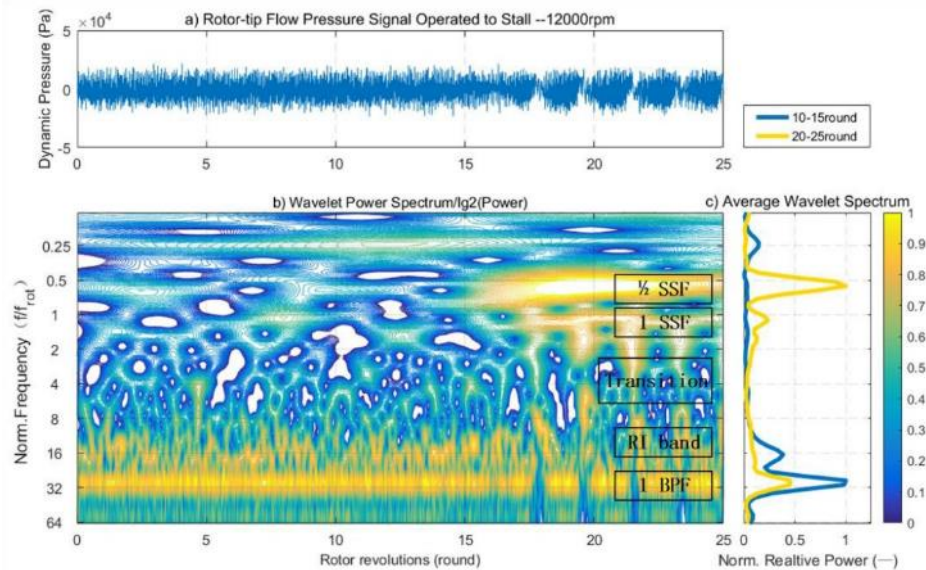
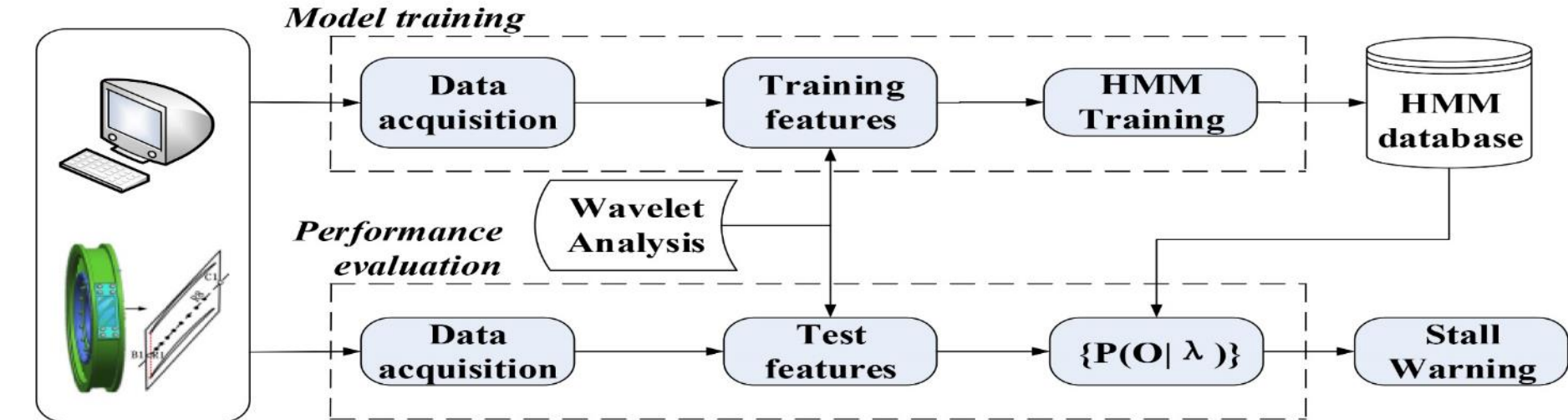
Acoustic Analogy: Tonal Noise



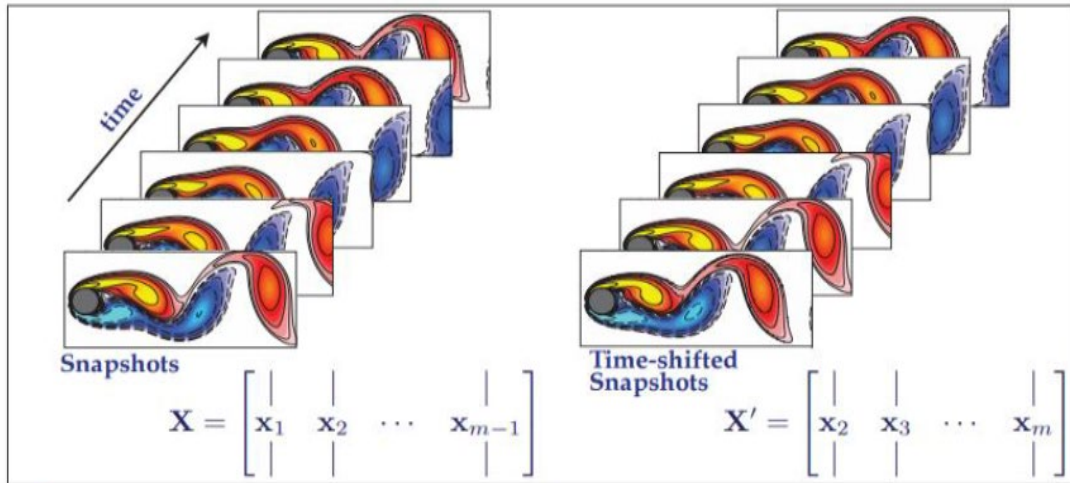
- Extract unsteady CFD data on the surface of the blade;
- Calculate unsteady aerodynamic forces on the surface of the blade;
- Calculate the sound source item (determine the rotating coordinate system, position, etc.);
- Solve the acoustic response equations at the BPF and at each Harmonic position;
- Calculate inlet sound field and post processing



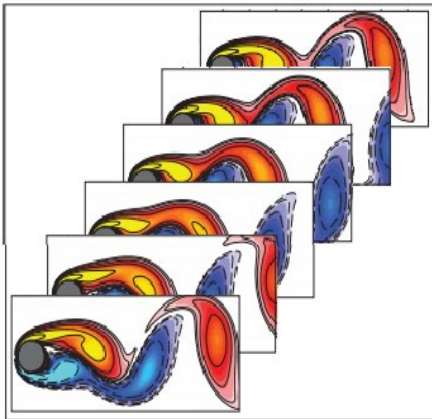
Application: stall warning



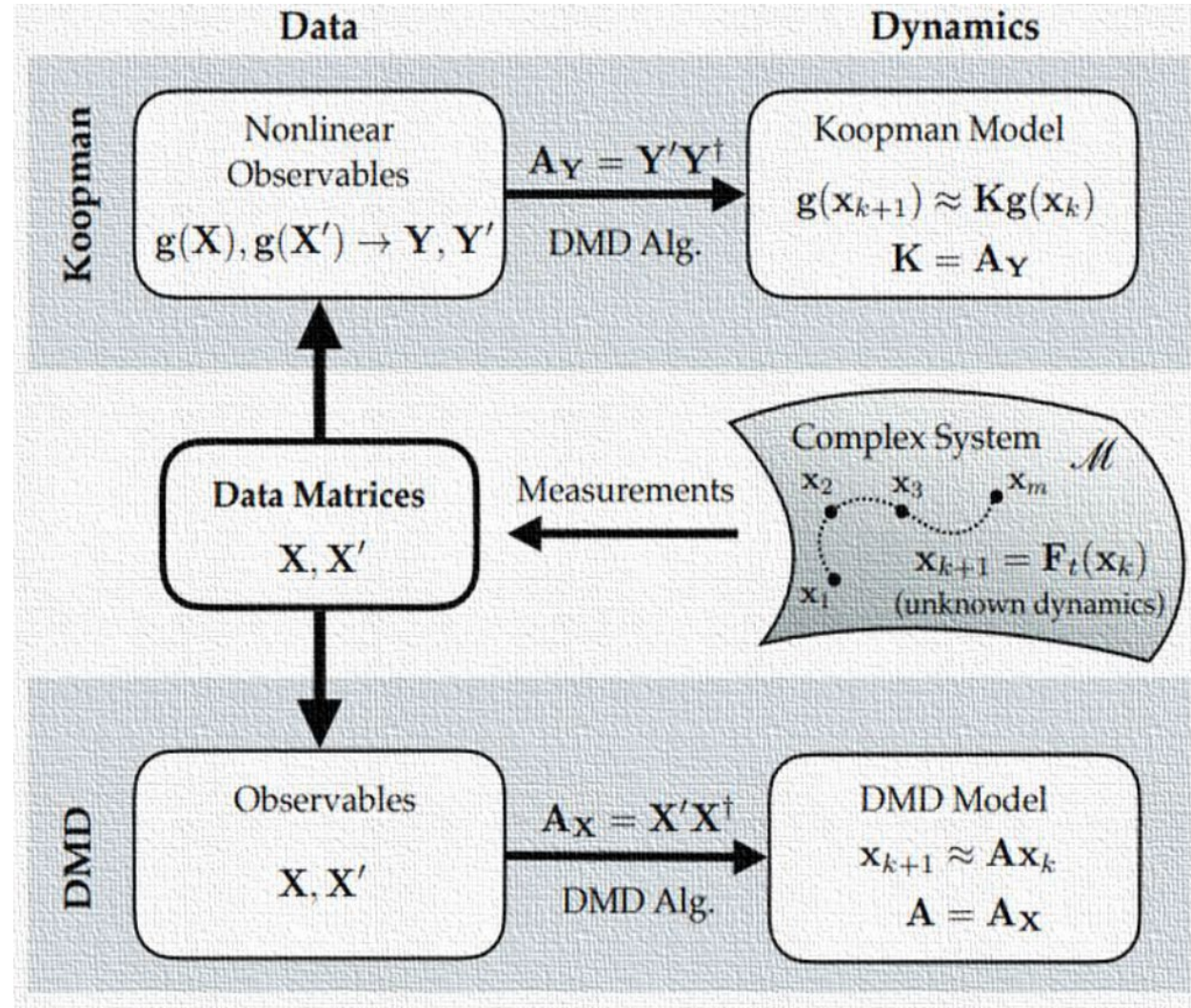
Application: Dynamic mode decomposition



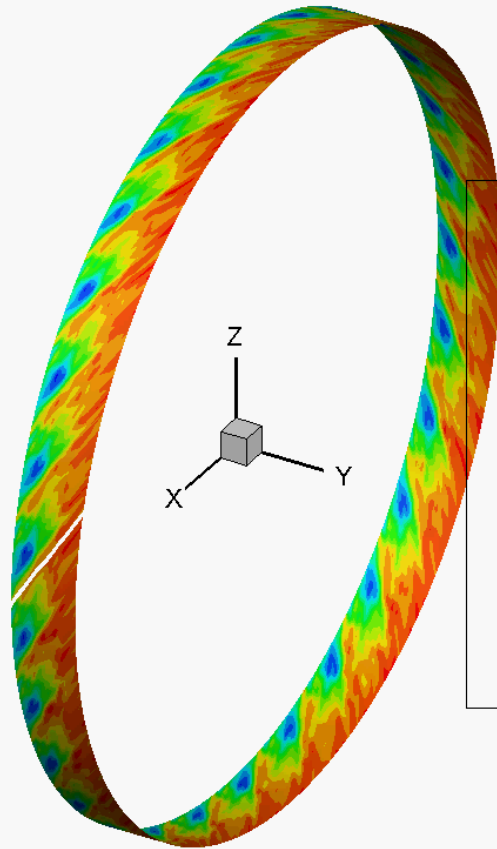
Predictive Reconstruction



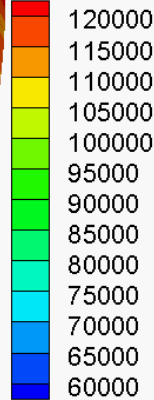
$$\mathbf{X} \approx \begin{bmatrix} | & | & \cdots & | \\ \phi_1 & \phi_2 & \cdots & \phi_m \\ | & | & \cdots & | \end{bmatrix} \begin{bmatrix} b_1 & 0 & \cdots \\ 0 & b_2 & \cdots \\ \vdots & \vdots & \ddots \end{bmatrix} \begin{bmatrix} 1 & \lambda_1 & \cdots & \lambda_1^{m-2} \\ 1 & \lambda_2 & \cdots & \lambda_2^{m-2} \\ \vdots & \vdots & \ddots & \vdots \end{bmatrix}$$



Application: Dynamic mode decomposition



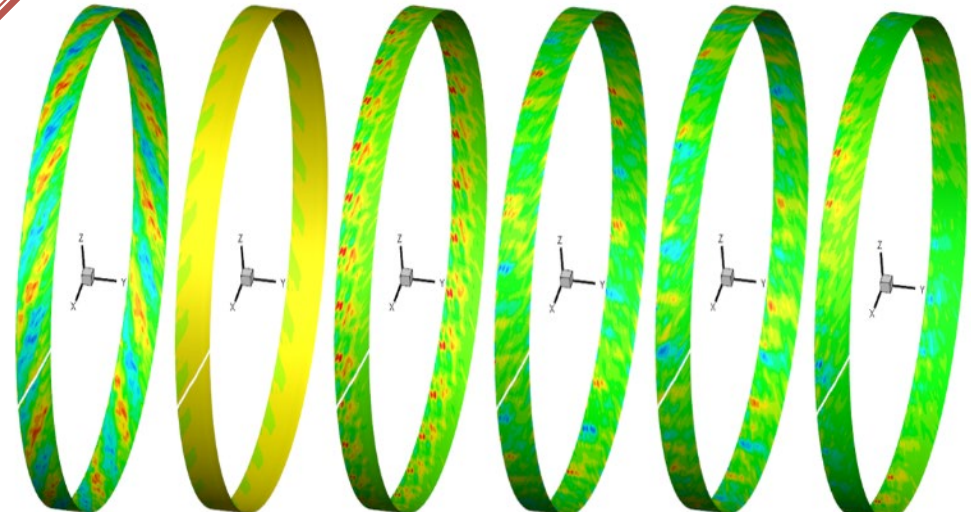
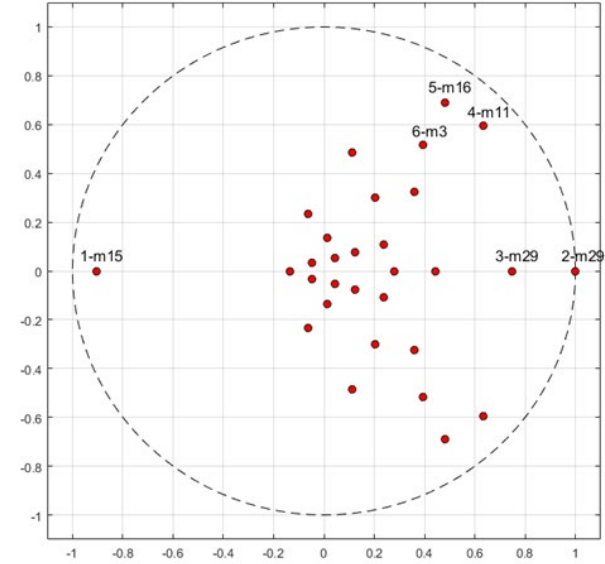
Tecplot(-15-12-)17000rpm-204800



$$\text{DMD: } [\lambda_k, \Phi] = \text{eig}(A/\rho)$$

特征值 λ_k

特征向量 Φ



1-m15

2-m29

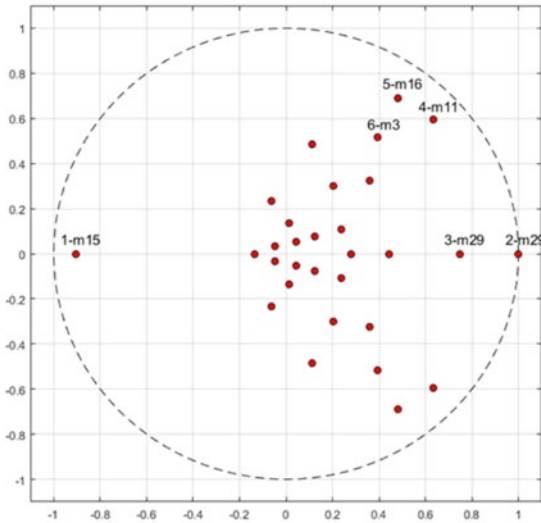
3-m16

4-m11

5-m16

6-m3

Application: Dynamic mode decomposition

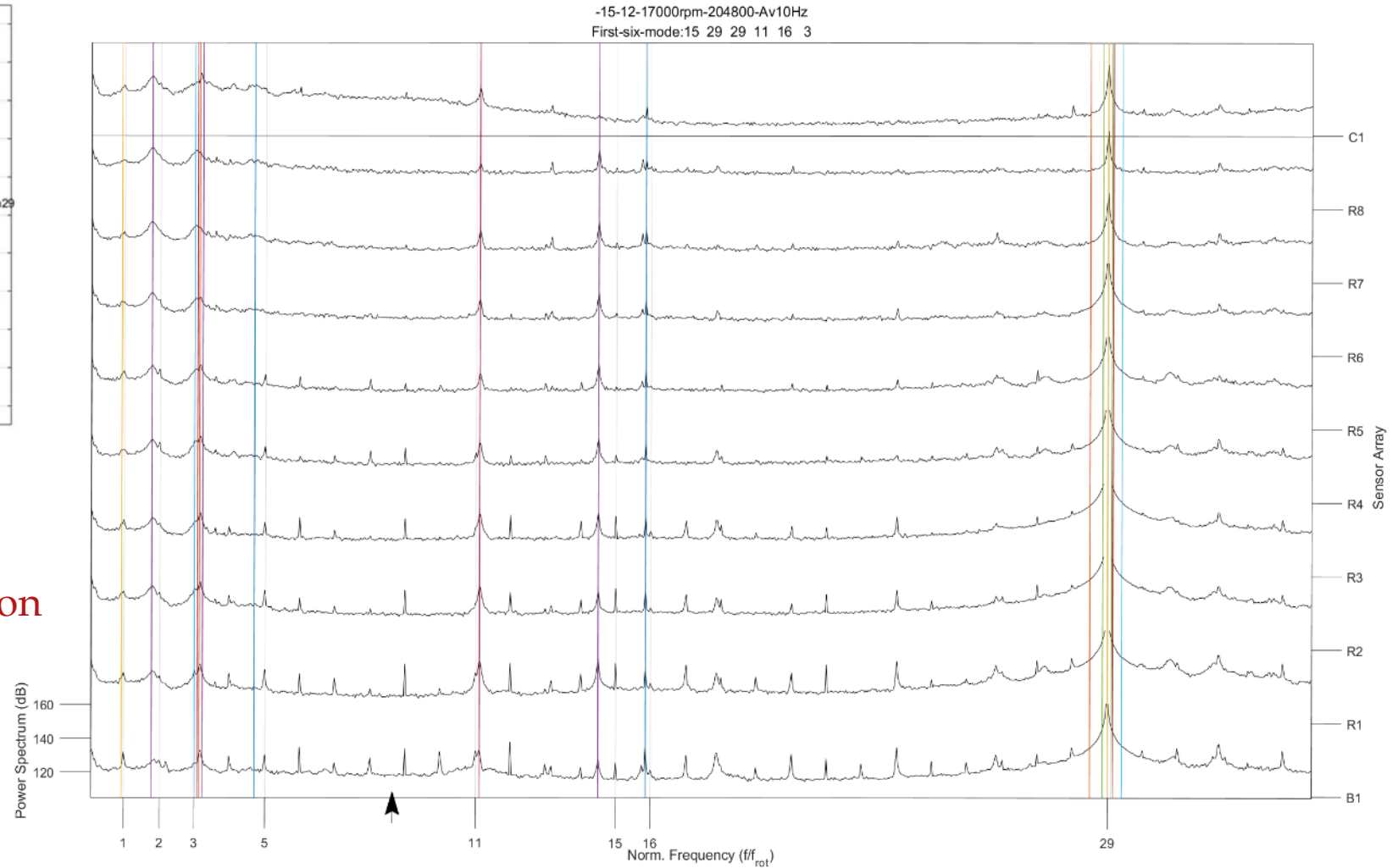


$$w_k = \ln(\lambda_k) / T$$

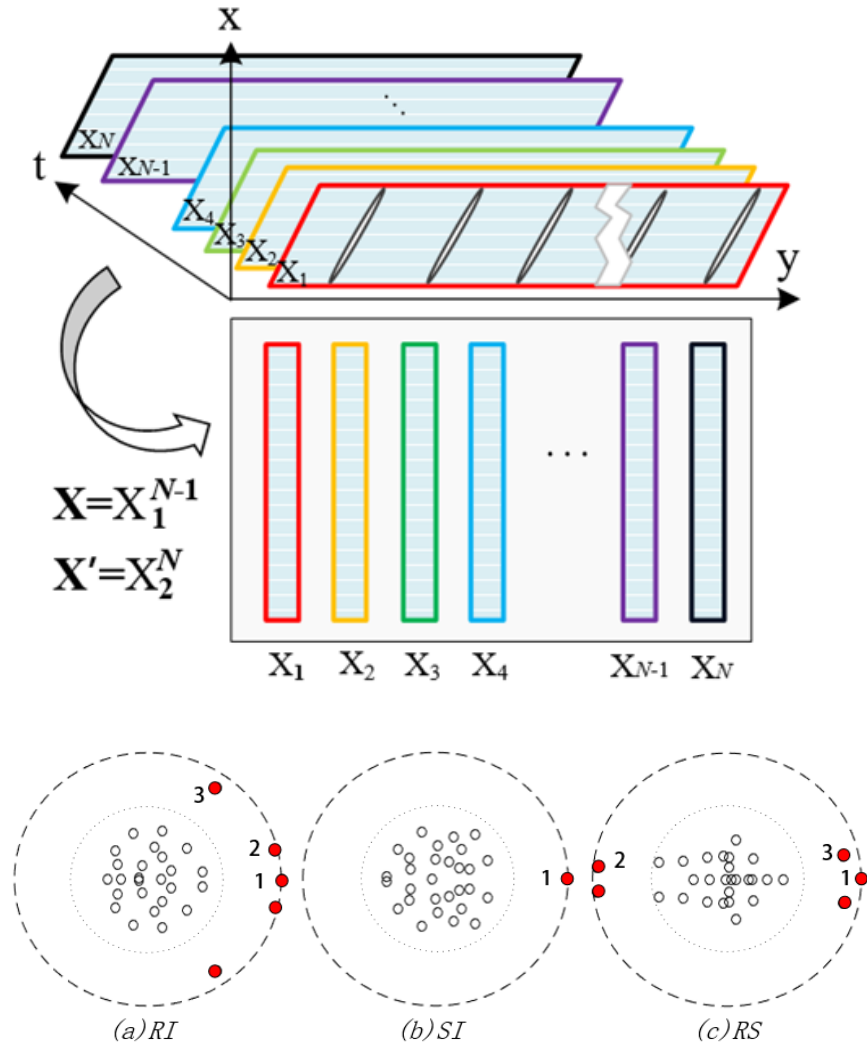
Coordinate system conversion

$$w = w_k \pm m * SSF$$

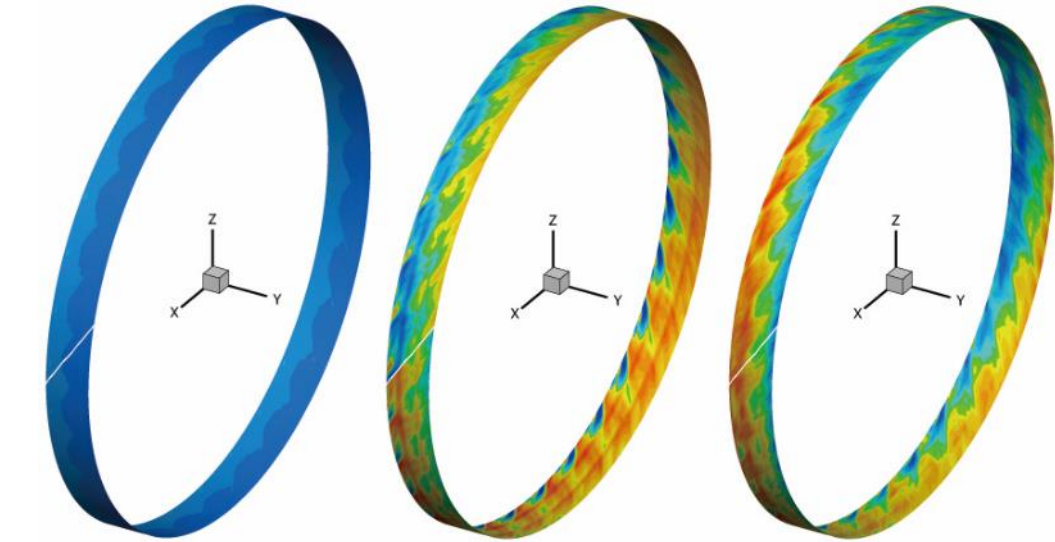
(Positive and negative corresponding modal rotation Positive and negative directions))



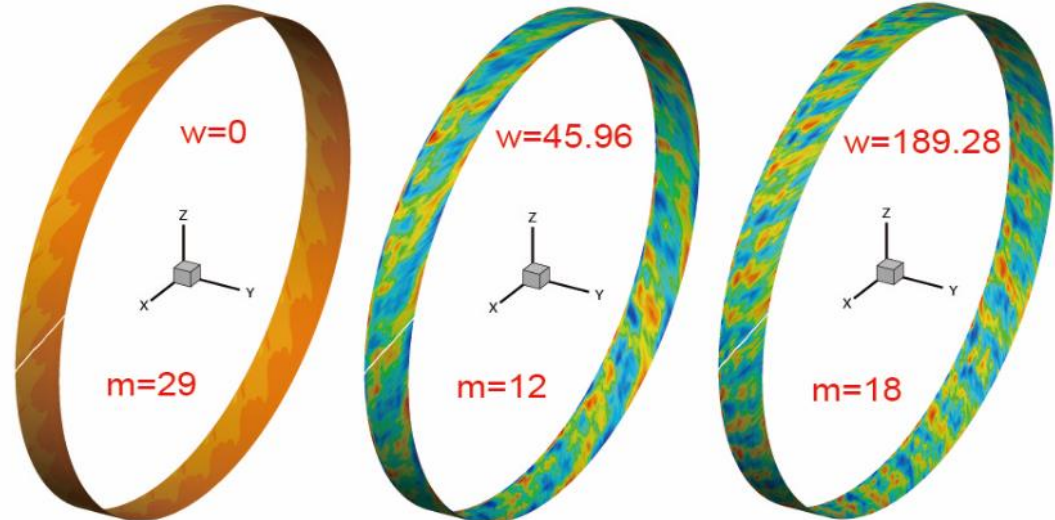
Application: Dynamic mode decomposition



RS



RI



Application: Mode detection



$$\frac{1}{c_0^2} \left(\frac{D}{Dt} \right)^2 p - \Delta p = 0$$

$$p_f(x, r, \theta, t) = \sum_{m=-\infty}^{+\infty} \sum_{n=0}^{+\infty} A_{mnf} E_{mn}(\kappa_{mn} r) e^{i(2\pi ft + m\theta - \zeta_{mn} x)}$$

$$E_{mn}(\kappa_{mn} r) = C_{mn} [J_m(\kappa_{mn} r) + Q_{mn} Y_m(\kappa_{mn} r)]$$



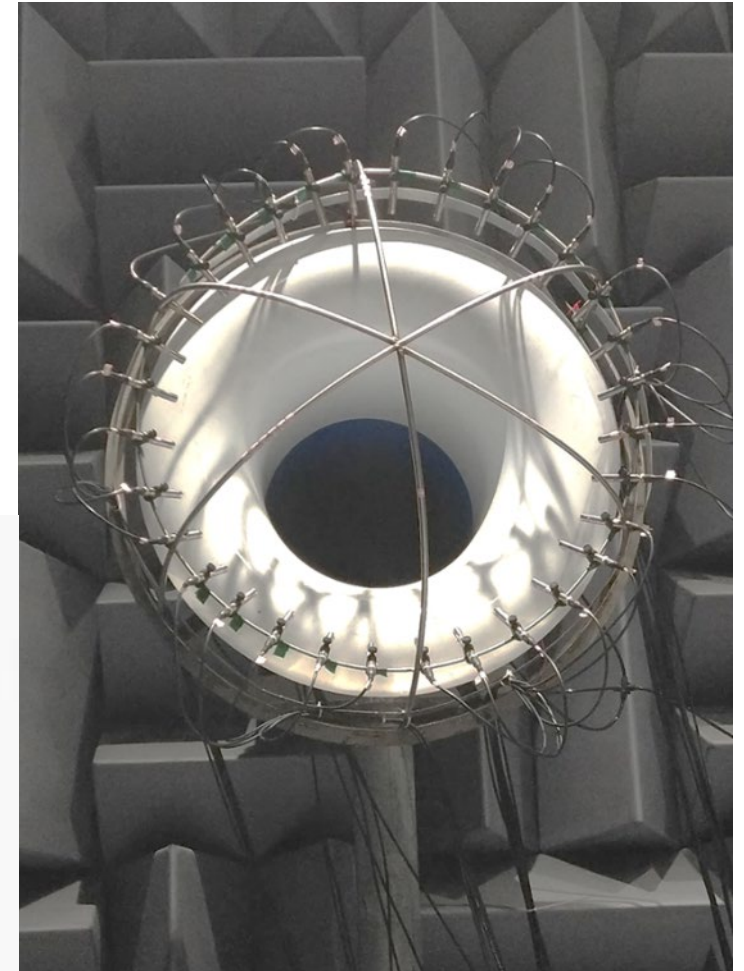
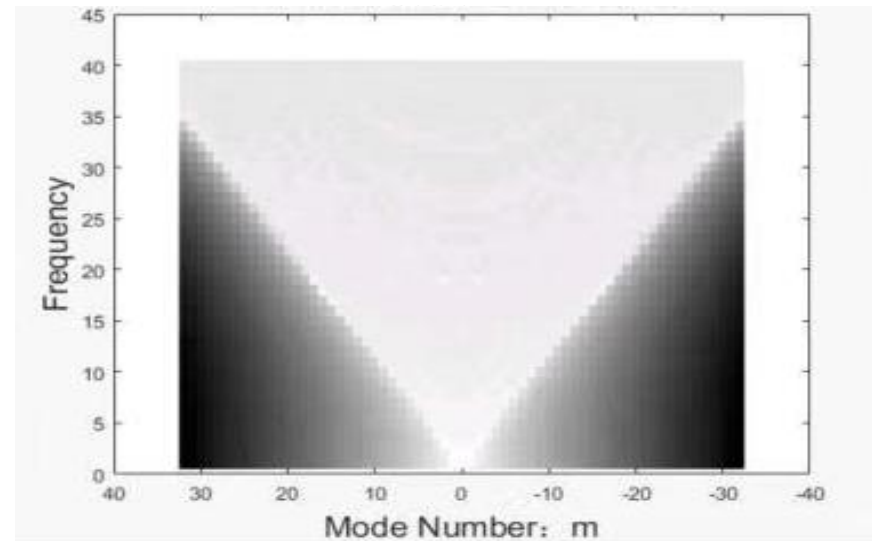
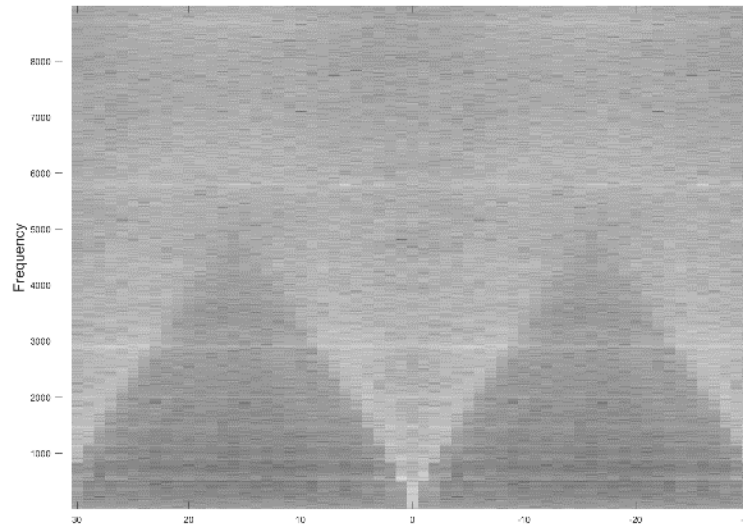
$$p_f(\theta) = \sum_{m=-\infty}^{+\infty} a_{mf} e^{-im\theta}$$

$$a_{mf} = \frac{1}{K} \sum_{k=1}^K p_f(\theta_k) e^{im\theta_k}$$

RMS

$$\Gamma_{mf} = \frac{1}{2} \left\langle |a_{mf}|^2 \right\rangle = \frac{1}{2K^2} \left\langle \sum_{k=1}^K \sum_{l=1}^K p_f(\theta_k) e^{im\theta_k} p_f(\theta_l) e^{-im\theta_l} \right\rangle =$$

$$\frac{1}{K^2} \sum_{k=1}^K \sum_{l=1}^K e^{im\theta_k} \left\langle p_f(\theta_k) p_f(\theta_l)^* \right\rangle e^{-im\theta_l} = \frac{1}{K^2} \sum_{k=1}^K \sum_{l=1}^K e^{im\theta_k} C_{kl} e^{-im\theta_l}$$

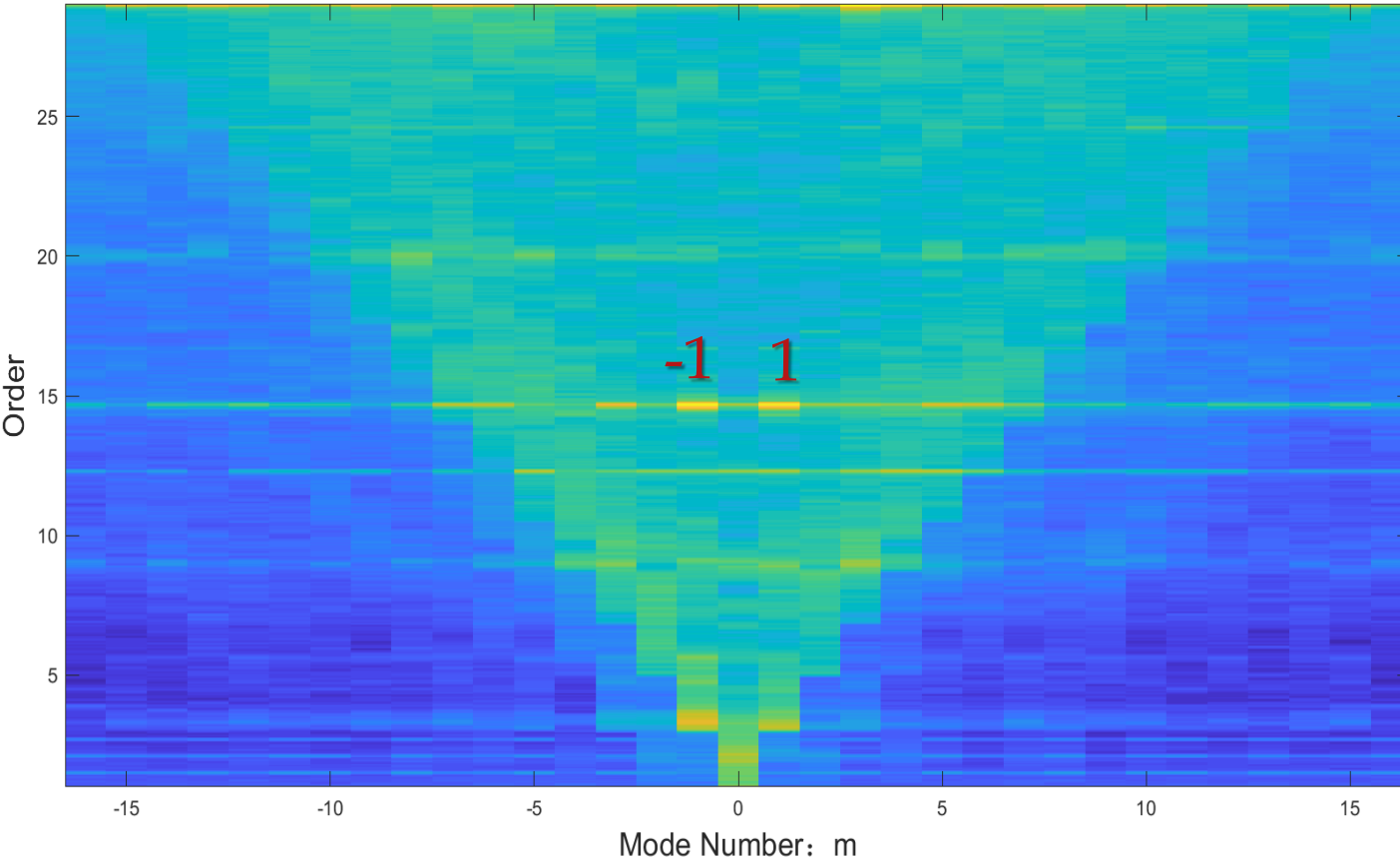


Application: Mode detection



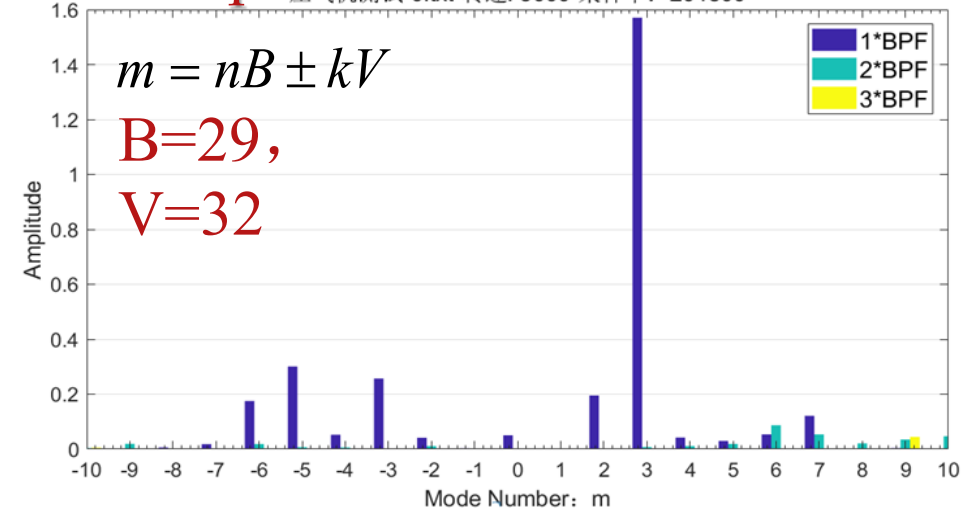
10000rpm

实验11-2018-05-09-截止模态分析 -CPSD method 2
升速2-23-t1-10000.mat-转速: 10000-采样率: 204800



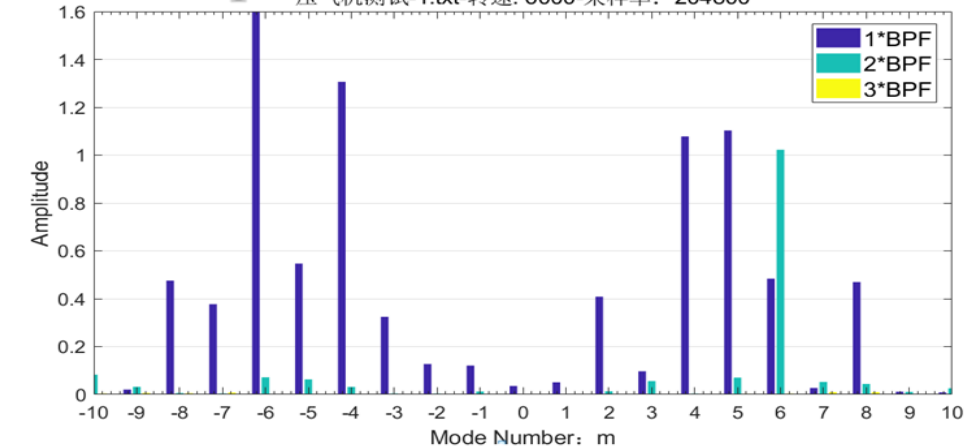
5000rpm

实验11-2017-05-10-模态分析
压气机测试-0.txt-转速: 5000-采样率: 204800



6000rpm

实验11-2017-05-10-模态分析
压气机测试-1.txt-转速: 6000-采样率: 204800





上海交通大学

SHANGHAI JIAO TONG UNIVERSITY

感谢聆听！